The Pennsylvania State University

The Graduate School

ACOUSTIC ANALYSIS OF COMPOUND HELICOPTERS WITH TRIM VARIATIONS

A Thesis in

Aerospace Engineering

by

Heather Marie Barron

Submitted in Partial Fulfillment
of the Requirements
for the Degree of

Master of Science

August 2013

The thesis of Heather Marie Barron was reviewed and approved* by the following:

Kenneth S. Brentner
Professor of Aerospace Engineering
Thesis Advisor

Joseph F. Horn
Associate Professor of Aerospace Engineering

George A. Lesieutre
Professor of Aerospace Engineering
Head of the Department of Aerospace Engineering

*Signatures are on file in the Graduate School

ABSTRACT

This thesis presents a prediction method that analyzes the acoustic radiation of compound helicopters when trim is varied. The goal of this thesis was to develop a method that uses added features such as a wing and an auxiliary propeller (described as added 'control degrees of freedom') on a compound rotorcraft to reduce the noise generated when flight conditions were changed. Noise radiation is an important factor for both military and civilian helicopters. There has been limited research on compound rotorcraft acoustics. Prior research focus has been primarily on tiltrotor configuration and large civil helicopter acoustics. For this thesis, a notional vehicle with a main rotor, tail rotor, wing, and auxiliary propeller was used. A flight simulation model and a noise prediction tool were coupled together to produce all of the analytic results. Predictions indicated that with the additional 'control degrees of freedom', the noise from a compound helicopter can be changed drastically.

Research showed that reducing the rotor advancing tip Mach number resulted in a large noise reduction in high-speed flight; this can be useful when finding an optimal noise flight condition. Results also showed that changing the thrust produced by an auxiliary propeller located aft of the aircraft does not have a dramatic effect on the overall sound due to the dominance of thickness noise in all areas around the aircraft. Even though noise does not change drastically with the change of thrust produced, the change is still crucial to the performance of the aircraft. Studies revealed that combining both advancing-tip Mach number changes along with thrust changes produced the best way to alter the noise produced from the aircraft. The dominant noise source in the cases run were from the auxiliary propeller. Independently changing the auxiliary propeller's tip Mach number drastically changed the noise produced by the rotorcraft and is the most effective way to reduce overall noise.

TABLE OF CONTENTS

LIST OF FIGURES

LIST OF TABLES

LIST OF SYMBOLS

c	Speed of sound in quiescent medium, m/s
ρ	Density of quiescent medium, kg/m^3
ρ'	Density of perturbation, kg/m^3
p'	Acoustic pressure, $p - p_0$, ($p' \approx c^2\rho'$, outside of source region), Pa
$f = 0$	Function that describes the source surface
dS	Element of acoustic data surface
t	Observer time, s
τ	Source time, s
x	Observer position vector, with components x_i, m
y	Source position vector, with components y_i, m
r	Distance between observer and source, **r** = $\|\boldsymbol{x} - \boldsymbol{y}\|$, m
P_{ij}	Compressive stress tensor, Pa
l_i	Components of local force intensity that act on the fluid, $l_i = P_{ij}n_j$, Pa
l_r	$l_i\hat{r}_i$, Pa
$\dot{l}_i$	$\dot{l}_i\hat{r}_i$, Pa/s
u_i	Components of local fluid velocity, m/s
v_n	Local normal velocity of source surface,$v_i\hat{n}_{i,\,\mathrm{m}}$/s
$\hat{n}_i$	Components of unit normal vector
$\dot{v}_n$	$\dot{v}_i\hat{n}_i$, ($\dot{v}_i = \partial v_i/\partial\tau$), m/s
$v_{\dot{n}}$	$v_i\dot{\hat{n}}_i$, ($\dot{\hat{n}}_i = \partial\hat{n}_i/\partial\tau$), m/s
M	Mach number of source with respect to a frame fixed to the undisturbed medium
$\dot{M}_i$	$\partial M_i/\partial\tau$

$\hat{r}_i$	Components of unit radiation vector
M_r	Mach number of source in radiation direction, $M_i\hat{r}_i$
$\dot{M}_r$	$\dot{M}_i\hat{r}_i$

Abbreviations

ABC	Advancing blade concept
BVI	Blade vortex interaction
BWI	Blade wake interaction
FW-H	Ffowcs Williams-Hawkings
HSI	High speed impulsive
N-S	Navier-Stokes
OASPL	Overall sound pressure level
RPM	Revolutions per minute
SPL	Sound pressure level
TPP	Tip path plane

Subscripts

ret	Quantity is evaluated at the retarded time, $\tau = t - r/c$
0	Denotes fluid variable in quiescent medium
T	Thickness noise components
L	Loading noise component
i	Array index denoting location in time
j	Array index denoting location in space

ACKNOWLEDGEMENTS

I would not be where I am today without the push from my parents. They have always told me to try my hardest, do the best I can, and to never give up. They have helped me emotionally and financially through my entire schooling and I couldn't be more thankful for everything they have done for me. To my mother, thank you for listening to me and telling me things could be worse. To my father, thanks for the extra engineering help. To my brother, thank you for telling me that I can do it myself and other people have no idea what they are talking about.

I would like to thank most my advisor Dr. Ken Brentner for his mentoring and his kindness. Every day he taught me something new and amazed me with his knowledge and insight (including life). His demand for perfection made me work a little bit harder, made me that much wiser, and made me learn a little bit faster so thanks for making me who I am.

My research could not have been finished without the help of previous students, specifically Ben Goldman, Taha Ozdemir, and everyone who worked on PSU-WOPWOP and GENHEL-PSU. Their longs hours made my work easier and without their countless hours of coding, this thesis could not be possible.

Without my friends I don't think I could have survived Penn State. Their advice and love kept me sane throughout the past few years. So thank you for telling me it will be OK and that in a few years I will laugh at all the things I cried about.

Lastly, I would like to thank my sponsors for providing funding for all of the research, they literally made this possible.

Chapter 1

Introduction

For years, conventional helicopters have been used for all types of tasks; search and rescue, military operations, or personnel transportation. Conventional helicopters excel in hovering and low to moderate forward flight speeds, but there is an increasing demand for helicopters to achieve better performance and higher speeds. In high-speed flight, helicopters encounter factors that limit the flight speed, including retreating blade stall, vibration levels, and excessive drag, therefore new configurations have been sought over the past few years to increase the capability of the helicopter in high-speed forward flight. One class of rotorcraft that is being investigated is a fully compounded rotorcraft. Such a configuration is characterized by the use of wings and an auxiliary propulsive device, which enables helicopters to achieve greater performance while overcoming the limiting factors afflicting conventional helicopters.

The noise produced by helicopters can be high enough to compromise their mission and utility. Both civil and military rotorcraft face increasingly stringent noise requirements. In particular, the military is concerned with noise radiation both at home and when deployed. Civil helicopters must meet noise certification and even stricter local community regulations. Specifically the FAA and ICAO have certification and operational requirements that these aircraft must abide to in order to protect communities from excessive noise exposure.

With new advancements in compound rotorcraft technologies constantly surfacing and the restrictions on noise for helicopters potentially changing, the need for prediction of rotor noise is an increasingly important component for the analysis and design of rotorcraft. It is advantageous for engineers to be able to predict the noise from aircraft before production in order

to reduce costs and avoid potential setbacks in manufacturing. With the use of several tools, the ability to calculate rotor noise is possible. Designers are now able to investigate a variety of rotorcraft configurations, operating conditions, and flight cases without the need for costly experiments.

1.1. Conventional Rotorcraft

A conventional helicopter typically has one main rotor and one tail rotor; some examples are shown in Figure 1-1. This type of helicopter has four main controls: collective blade pitch, longitudinal and lateral cyclic, and tail rotor collective blade pitch. In order to maintain steady forward flight, a combination of these controls is required. The upward force of lift is obtained when the net force from the rotor remains opposite of the gravity force; similarly, forward (or backwards or sideways) propulsion is achieved by tilting the net force vector in the required direction [**1**]. The forward speed of conventional helicopters is limited due to retreating blade stall, thrust required, and vibration levels. As the aircraft flies forward, the airflow produced on each blade is different. Because of this, the rotor disk is divided into two sides during forward flight. On the advancing side, the blades rotate forward so the rotational speed and forward flight speed will add together. On the retreating side, the vehicle forward speed is in the opposite direction from the rotational speed, so the net speed is reduced. The difference in velocity on the advancing and retreating blades would result in an unbalanced lift on each side of the rotor and a rolling moment, if it were not corrected by cyclic pitch of the rotor blades. Cyclic pitch balances the lift by reducing the angle of attack on the advancing side of the rotor and increasing the angle of attack on the retreating side of the rotor. As the helicopter flies at increased forward speeds, eventually the increased angle of attack on the retreating side of the rotor results in blade stall, and on the advancing side of the rotor high-speed, transonic flow and increased drag.

Furthermore, at higher speeds, rotors typically experience dramatically higher vibration levels. Severe vibrations may eventually lead to damage of the rotor system and aircraft (if the pilot is even willing to fly with such vibration levels) [**2**] [**3**]. The high parasitic drag of the rotor hub and other parts of the fuselage in high-speed flight leads to poor lift-to-drag ratio for the helicopter. Both vibration and higher drag levels limit the maximum flight speed of conventional helicopters to level-flight cruises speeds of about 150 knots and dash speeds up to 200 knots with unrefueled ranges less than 500 miles. Higher flight speeds are possible with different helicopter configurations. The need for an aircraft that has vertical takeoff and landing (VTOL) capability along with high cruise speeds has led to some designs such as compound rotorcraft, advancing blade concept, and tiltrotor/tiltwing configurations [**4**].

Figure 1-1. Conventional helicopter examples (Left: Bell 407, Right: Sikorsky UH-60 Black Hawk).

1.2. Overcoming Limitations

1.2.1. Compound Rotorcraft

In order to achieve higher speeds, something must be done to reduce the problems associated with conventional helicopters. One approach is known as the compound rotorcraft. In

the early stages of compound rotorcraft design, the definition of compound rotorcraft was quite vague. In order to be classified as such, the aircraft had to have wings or an auxiliary thruster, most of the time having both. In today's terminology, a helicopter that has an extra source of lift and extra propulsive device is referred to as a fully compounded helicopter. Some examples of compound rotorcraft are shown in Figure 1-2 [**3**].

Figure 1-2. Compound helicopter examples (Left: Lockheed AH-56 Cheyenne, Right: Eurocopter X3).

1.2.1.1. Lift Compounding

By adding a wing to the fuselage of a helicopter, the main rotor does not need to provide all of the lift, but can be offloaded because at higher speeds the wing provides increasing amounts of lift. This will alleviate retreating blade stall and allow for increased speed. The addition of a wing comes with additional weight. Furthermore, though the main rotor no longer needs to produce as much thrust to provide the lift, the main rotor must still generate all the forward propulsive force. In order to do this, the main rotor disk must be tilted forward and this requires an increase in cyclic pitch, which tends to negate the benefits of a reduction in rotor thrust [**2**]. Also, the download on the wing created in hover may severely impact the payload capability of the aircraft. Finally, on a positive note, the wing has the advantage of providing storage for extra

fuel. Overall, the addition of a wing may provide a slight improvement in forward flight speeds, but for even faster speeds, it would be necessary to add an auxiliary propulsion device [**3**] [**5**].

1.2.1.2. Thrust Compounding

By adding an auxiliary propulsion device, the main rotor no longer needs to produce the majority of horizontal thrust in forward flight. Some examples of auxiliary propulsion devices are an added propeller, a turbo jet, turbo fan, or a ducted fan [**5**]. The main benefits of adding a thrust component is the ability to unload the main rotor at higher speeds, reduce vibrations, and increased fatigue life on components. These advantages come from the reduction of the main rotor forward tilt. With the incident angle on the fuselage lowered, there will be smaller cyclic loads, thus less power being applied to the rotor and less anti-torque required. Even though the power is reduced, this is offset by the power needed to run the auxiliary propeller [**2**]. Also, with the addition of a propulsive device, there is the addition of weight, mechanical complexity, and additional noise sources [**3**].

1.2.1.3. Full Compounding

To achieve highest speeds and best performance, it would be advantageous to add both lifting and thrusting components. This allows the lift and propulsive forces to be offloaded from the main rotor, reducing many of the problems that currently are associated with conventional helicopters. With both components, the forwards disk tilt of the main rotor is not required and the benefits of offloading the main rotor can be used to its full potential. This type of compounding is the most common and some examples of aircraft that have been manufactured are the Lockheed AH-56 Cheyenne and Eurocopter X3 [**2**] [**3**].

1.2.2. Advancing Blade Concept

In the mid 1960's, many companies were trying to developed new technologies to increase the speed of conventional helicopters. As shown in previous sections, most of these were compound rotorcrafts. Specifically, Sikorsky was experimenting with a compound rotorcraft, the S-61F/NH-3, and at the same time they created an alternative to compound rotorcraft called the Advancing Blade Concept or ABC. Examples of this type of aircraft are shown in Figure 1-3. The idea was to eliminate retreating blade stall at high speeds by using two counter-rotating rotors so that when stall occurred on the retreating blade, it would occur simultaneously on both blade, balancing the forces. Earlier co-axial helicopters were developed, but primarily for compactness and the elimination of the tail rotor, although no thought of ABC was considered [**6**].

Figure 1-3. Advancing Blade Concept Examples (Left: Technology Demonstrator XH-59A, Right: Sikorsky X-2)

With this rotor configuration, the rotor's capability to generate lift would not drop off with speed or altitude, this was a huge breakthrough in helicopter technology. The biggest challenge in manufacturing this aircraft was the construction of the rotor blades due to their unique geometry, specific material needed, and use of rigid blades. The first flight of an ABC

aircraft was in June, 1973. Since then, extreme advances in controls and handling qualities along with structural enhancements have been made on ABC models. Some models included auxiliary propulsion devices such as side mounted jets and aft mounted propellers. Thirty years after the first flight of an ABC helicopter, such advances in blade construction, shape and airfoil design, vibration control, propulsion systems integration, and fly-by-wire controls allowed Sikorsky to return back to the ABC concept and develop the X-2 high speed aircraft (Right in Figure 1-3). This aircraft achieved a flight speed of 250 knots in 2010 and won the Collier Trophy in 2010 for the greatest achievement in aeronautics in America with respect to improving performance, efficiency, and safety of air vehicles within the preceding year. The ABC concept will continue to be used and improved and will likely become a part of the next generation of high-speed helicopters [**6**].

1.2.3. Tiltrotor/Tiltwing

Another way to overcome the speed limitations of a conventional helicopter is to change the direction of the forces being produced during flight. A tiltrotor aircraft takes off and lands vertically, like a conventional helicopter, with the rotors oriented horizontally. As the aircraft gains forward flight speed, the wing tip-mounted rotors can tilt to resemble fixed wing turboprop aircraft. In this configuration, the vehicle can achieve flight speeds of about 300 knots. Some examples of tiltrotor helicopters are shown in Figure 1-4. The rotors on tiltrotors typically cannot be as large as those of a helicopter, so the hovering efficiency is not as high as a conventional helicopter. On the V-22, the rotor diameter is limited by the need to operate and hanger the aircraft on an aircraft carrier [**4**].

Figure 1-4. Tiltrotor helicopter (Left: Bell-Boeing V-22 Osprey, Right: Bell XV-15)

A configuration similar to the tiltrotor, is the tiltwing. The idea is the wing can be tilted from the normal fly position with propellers providing forward trust to a vertical position with the propellers providing vertical lift. With this configuration, pilots would have problems controlling the aircraft because the wing would stall constantly during conversion from VTOL to turboprop configuration. For this and other reasons, the tiltwing concept never became a replacement for a conventional helicopter. Some examples of tiltwing aircraft prototypes are shown in Figure 1-5.

Figure 1-5. Tiltwing helicopter (Left: Hiller X-18, Right: Vertol VZ-2)

Tiltwing and tiltrotor aircraft have tradeoffs between lift and thrust that must be analyzed when it comes to forward flight. The ideal window of trim encompasses the ability to fly at speeds comparable to fixed wing planes while also being able to achieve vertical takeoff and

landings. The potential for faster speeds comes at a price and at the expense of payloads; tiltrotors do not have the same transport efficiency of a helicopter. Furthermore, there is increased mechanical complicity and increased weight with the new hardware. However, the ability to fly at higher speeds overcomes most of these disadvantages [**4**].

1.3. Problem Description

Helicopters are extremely complex aeromechanical vehicles with hundreds of moving parts. The aerodynamic environment in which the aircraft is flying is complex and is fundamentally unsteady. Each of the various components (specifically rotors for this thesis) generate their own noise and there may be both aerodynamic and acoustic interactions between the different components. Helicopter rotor noise can be classified into several distinct categories: discrete frequency noise, which consists of thickness and loading noise, blade-vortex interaction noise, and high speed impulsive noise. Similarly, broadband noise consists of non-deterministic loading noise, turbulence ingestion noise, blade-wake interaction noise, and blade self-noise [**7**]. Some other sources of noise include the tail rotor noise which can be subjectively more important than main rotor noise and for a compound configuration, the auxiliary propeller which acts similar to the tail rotor noise. Lastly, there are noise sources such as the engine, drivetrain, or gear noise.

1.3.1. Discrete Frequency Noise

Helicopter rotor noise tends to be focused at harmonics of the main rotor blade passage frequency. This is because there is a periodic nature of the rotor rotation when it is seen in a nonrotating frame. Discrete frequency noise consists of rotational noise, blade-vortex interaction

(BVI) noise and high-speed impulsive noise. Rotational noise is made up of thickness and loading noise and they are related to linear aerodynamic theory. Thickness noise is due to the displacement of the fluid by the rotor blade in the flow field. By periodically pushing the air aside, each blade produces a pressure disturbance. Thickness noise is primarily focused in-plane of the rotor. Sound pressure is related to the blade lift and thickness, so if there is more than one blade, the sources can be evaluated separately then added together [**8**]. Loading noise is due to the acceleration of a force on the air around the object (in this case the blade). The term, designated as 'loading noise', usually refers to the harmonic noise from non-impulsive loading sources. Loading noise is generally directed below the rotor [**7**] [**9**].

Blade-vortex interaction noise is generated due to the shed tip vortices interacting with a subsequent blade. This causes a rapid, impulsive change in the loading on the blade which results in a highly directional type of noise. BVI can happen on the advancing and retreating side of the rotor disk and the directivity is categorized by its orientation. If BVI is occurring on the advancing blade, the noise is directed down and forward of the aircraft, while if it is occurring on the retreating blade, it is directed down and aft of the aircraft. In some flight regimes (specifically forward descent), BVI occurs continuously. This type of noise is very loud and annoying to nearby communities and should be avoided as much as possible [**7**].

At high rotor tip speeds, the rotor will generate high-intensity impulsive noise in the direction in-plane of the rotor, which is called high-speed impulsive (HSI) noise. The peak levels of noise on helicopters normally occur in the forward region of the aircraft; this is predominantly due to thickness and HSI noise. HSI noise is related to the transonic flow around the blade and is caused by transonic flow shock formation on the advancing rotor blade. As the advancing tip Mach number increases, this sound will become the dominate noise and be particularly intense and annoying [**9**]. Figure 1-6 shows the directivity of the various types of noise produced by the rotor.

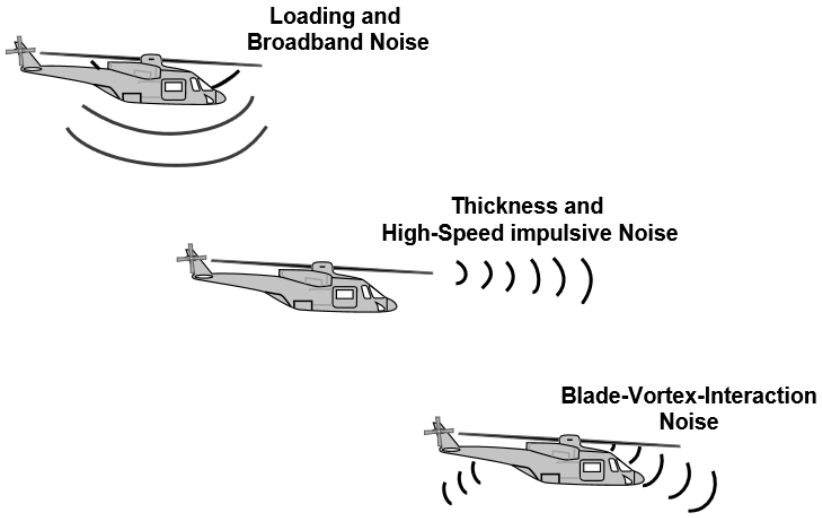

Figure 1-6. Directivity from various rotor noise sources (from Brentner and Farassat [**7**])

1.3.2. Broadband Noise

The frequencies in which broadband noise contributions fall into are in the range where human hearing is most sensitive so the contribution broadband noise makes to the overall noise can be considerable. Broadband noise consists of stochastic and non-deterministic loading noise sources that are essentially generated by random loading on the rotor blades. These noise sources are classified as turbulence ingestion noise, blade-wake interaction (BWI) noise, and blade self-noise. When turbulence is present in the flow, any interaction with the blade surface can generate broadband noise. This can be described as turbulence ingestion noise and can produce both narrow-band and broadband noise. It can occur naturally in the atmosphere or as a reaction from the blade wakes themselves [**9**] [**10**].

The middle frequency broadband noise is produced by blade wake interaction. BWI is due to the blade interaction with the wake turbulence created from the previous blades. It is produced by the blade's leading edge loading noise reaction to the turbulence encounters. Figure

1-7 shows the flow characteristics for broadband frequency noise. In this figure, the tip of a blade is shown interacting with a flow field resulting in tip vortices (these are represented by vortex tubes) and a detailed explanation on how BWI is produced can be seen. BWI appears in level flight and mild climb conditions [**10**].

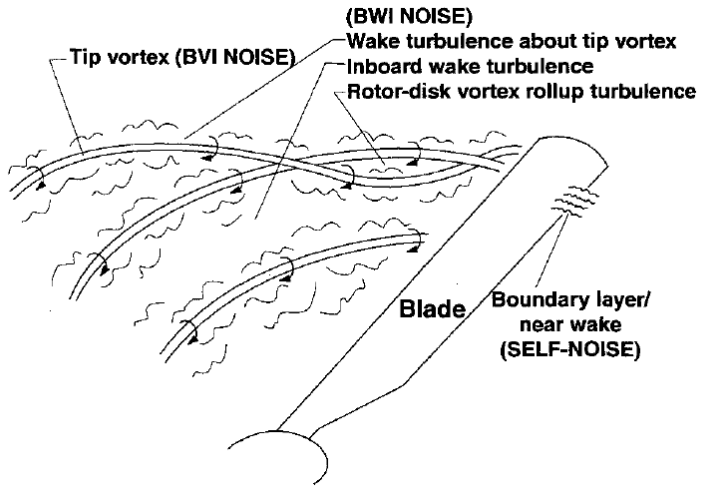

Figure 1-7. An illustration of flow the flow field a rotor blade encounters (from Brooks and Burley [**10**]).

The last type of broadband noise is called blade self-noise; it occurs on the blade itself due to turbulence in the boundary layer or related to flow separation and shedding. It is predominantly trailing edge noise and is a result of scattering of the turbulent pressure field from the passage of turbulence over the sharp trailing edge into the near-wake. Blade self-noise is generated by several mechanism as shown in Figure 1-8; these include turbulent boundary layer or separated flow interaction with the edge, laminar boundary layer vortex shedding, and blade tip noise [**10**].

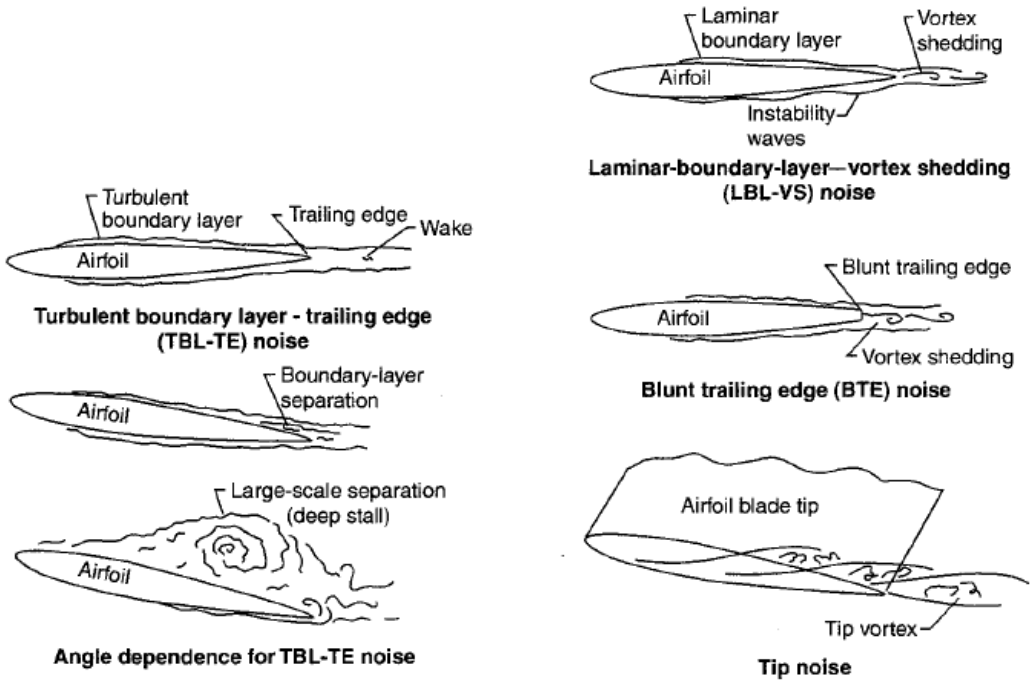

Figure 1-8. An illustration of flow conditions producing blade self-noise (from Brooks and Burley [**10**]).

1.3.3. Tail and Auxiliary Propeller Noise

On most helicopters, the noise produced by the tail rotor is the most noticeable and disturbing. The tail rotor noise mechanisms are the same as the main rotor mechanisms, but the tail rotor has a higher fundamental frequency. On a compound rotorcraft, there may be an auxiliary propeller that seems similar to a tail rotor, but in most cases the auxiliary propeller performs at much higher RPM's so its fundamental frequency is the highest of all the rotors. The broadband noise and discrete frequency noise of the tail rotor and auxiliary propellers are produced in the same manner as the main rotor; the major difference is the directivity with respect to the observer of each source. An additional source of noise from the tail rotor and auxiliary propeller is the interaction of the wakes from the main rotor. This interaction noise is due to the

unsteady loading resulting from interactions with distorted inflow or the wakes entering the rotor or propeller [**8**].

1.3.4. Miscellaneous Noise

The rotors of a helicopter are not the only noise generators on a helicopter. Mechanical components and external devices can also create noise. The helicopter transmission and engine are sources of high frequency sound, but these are only important for the internal and near field noise predictions. Noise from the drivetrain and gears can be heard distinctively, but for rotorcraft noise predictions in this thesis, these types of sounds are not considered because they do not have the same impact as the rotors do in the far field.

1.5. Previous Research

There has been limited research on the specific topic of compound rotorcraft acoustics (at least that is available to the public). The main research interest has been in tiltrotor acoustics and quiet, powered-lift propulsion acoustics. Their major focus has been in terminal area operations and how shifting the rotor TPP affects blade vortex interaction noise. Research on acoustics of the XV-15 was done by NASA, the Army, and Bell Helicopter Textron, Inc. They evaluated the noise reduction potential for a specific tiltrotor aircraft. Flight tests were done to gather the lowest noise approach profiles [**11**]. Conner and Wellman have performed experiments to investigate the far-field hover acoustic characteristics of the tiltrotor XV-15 with advanced technology blades [**12**]. Similarly, Maisel, Guilianetti, and Dugan performed noise experiments with the XV-15. They discuss the design phase from start to finish of the rotorcraft. They investigated rotor downwash and noise and possible operation methods to reduce noise [**13**].

Research on quiet power-lift aircraft was performed by NASA. Although the research used a fixed wing aircraft, the ability to have a short take off is needed to reduce traffic density at airports. These aircraft would need to be able to perform on short runways so the use of powered-lift type of aircraft would be required, specifically the aircraft would have to employ some sort of engine thrust (tilting the engines or creating downwash) to help provide lift. The program was initiated to develop a suitable propulsion technology base for short-haul powered-lift aircraft and research emphasis was on low noise, low exhaust emissions, and high performance [**14**].

Russell and Johnson performed a study on the noise from notional large civil compound helicopters. Specifically, very large conventional and compound rotorcrafts, and tiltrotor aircraft were analyzed. The main focus of their paper was to see how the compound rotorcraft performs when it is compared to a conventional helicopter and tiltrotors by using design missions that is shorter than optimum for a tiltrotor and longer than optimum for a conventional helicopter [**15**].

Overall, not much research has been done specifically on compound rotorcraft acoustics. The studies have primarily been on tiltrotor and large conventional helicopters. Because compound rotorcraft seem to be the future of high-speed flight vehicles, it would be beneficial to preform acoustic research on them. This thesis provides low fidelity research on compound rotorcrafts.

1.6. Reader's Guide

The remainder of this thesis is organized as follows:

- **Chapter 2** provides background on the programs used in this thesis. Specifically the flight dynamic model GENHEL-PSU and the acoustic theories and formulations used in aeroacoustic prediction code PSU-WOPWOP.

- **Chapter 3** describes the results when different trim parameters are varied.
- **Chapter 4** summarizes the results of this research and offers recommendations for future work.

Chapter 2

Approach

2.1. Overall Strategy

During the design phase of a helicopter, analysis tools, such as flight simulators and noise prediction codes, can be very helpful for keeping costs low and providing detailed information about the aircraft design. These tools give the designer some indication of how design changes and operating procedures can affect the aircraft without running costly scaled experiments. For this thesis, two analysis tools are being combined to generate the noise produced by a compound rotorcraft. The first program, PSU-WOPWOP, is a rotor noise prediction code. It uses Farassat's Formulation 1A of the Ffowcs Williams-Hawkings equation and requires two sets of data: the loading data on the blades and the surface geometry for the rotor blades. The loading data comes from the other program used in this work, GENHEL-PSU. GENHEL-PSU is a non-linear, blade element, flight dynamic model. This program requires user defined input in the form of flight conditions and requires all of the dimensions and specifications of the aircraft. The blade surface geometry is generated by a third tool known as BladeMaker. BladeMaker is discussed in more detail in Appendix C. Figure 2-1 shows a flow chart of how these tools are coupled together in order to perform the noise prediction.

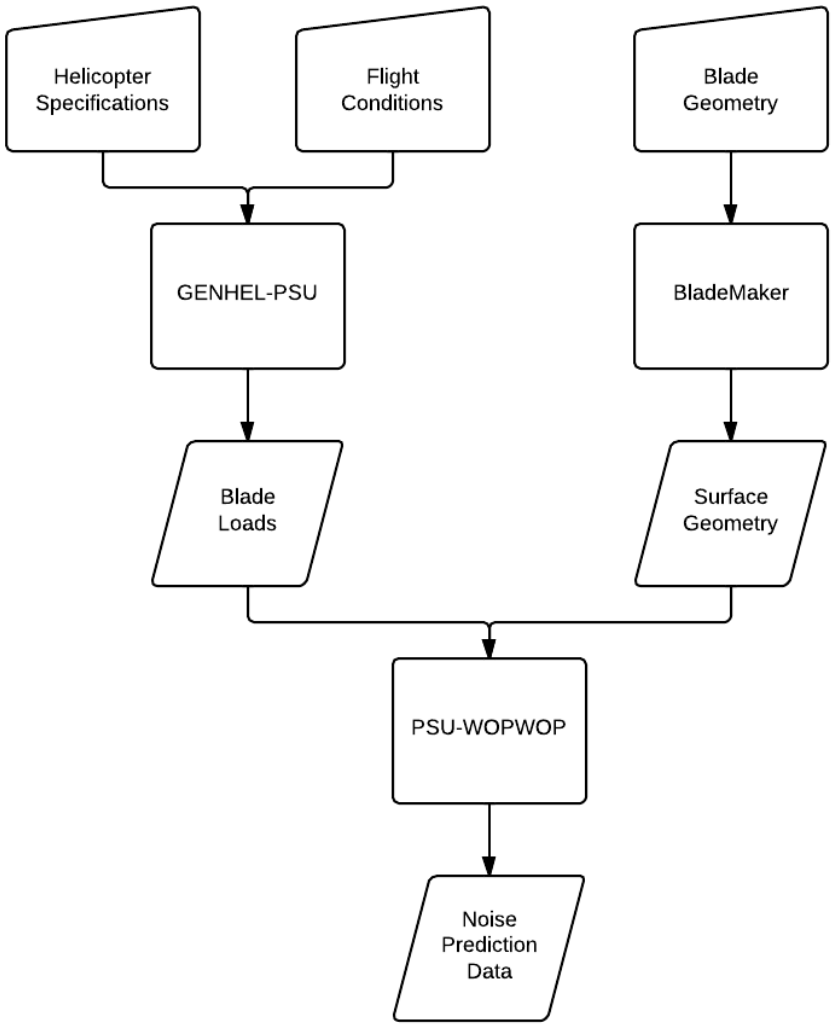

Figure 2-1. Flow chart of approach

2.2. Rotor Loading Model

The noise prediction software PSU-WOPWOP requires blade motion and loading information for each rotor to calculate noise from each rotor. This information is calculated by the program GENHEL-PSU. This program is complex and requires detailed specification and dimension of the aircraft.

2.2.1. GENHEL-PSU Overview

GENHEL-PSU is a simulation based loosely upon the UH-60A. The configuration has been described later in the Thesis Configuration Description, but overall it is a compound somewhat similar to the UH-60A with an added wing and aft mounted auxiliary propeller. The pitch of the blades on the auxiliary propeller can be controlled to allow for an increase or decrease in thrust. GENHEL-PSU is a Penn State derivative of the U.S. Army AFDD *GEN*eral *HELI*copter Flight Dynamics Simulation (GENHEL) computer program. For the model, this program provides a non-linear mathematical model of a compound helicopter (Note: the rotor blades used for the acoustic model are NOT UH-60A rotor blades, but rather blades with rectangular plan form). Originally it was created for engineering analysis then developed to allow piloted simulations. The model allows six 'degrees of freedom' and generates a detailed model of rotor hub geometry, lag dampers, and pitch control mechanisms. The program is written using FORTRAN subroutines and the primary modules include main rotor, tail rotor, fuselage loads, horizontal and vertical tails, and engines. Lastly, GENHEL-PSU is able to interface with MATLAB/Simulink software environment [**3**] [**16**].

2.2.1.1. Design

Significant care has been taken into account to provide the ability to calculate all forces and moments on the simulation helicopter. GENHEL-PSU has been modified to include user defined control laws for roll, pitch, yaw, heave, and rotor RPM in place of the existing typical stability augmentation systems and the engine electric control units, enabling the study of a wide array of cases, such as steady flight, perturbations, or sweeping of specified controls [**16**].

Some additional features of GENHEL-PSU include a blade element rotor model that includes time marching solution of rigid blade flap and lag dynamics plus a quasi-steady model of first torsion mode. GENHEL-PSU uses the three state Pitt-Peters inflow model and includes non-linear look up tables for blade section coefficients of lift and drag as a function of angle of attack and Mach number. Similarly, there are look up tables for fuselage aerodynamic loads based on wind tunnel data. The tail rotor uses the Bailey model and the auxiliary propeller uses look up tables for the lift, drag, and pitching moment coefficient [**16**] [**17**] [**18**].

GENHEL-PSU is implemented in the fixed-base flight simulator located in the Vertical Lift Research Center of Excellence and is used to simulate dynamic maneuvers with numerous trim solutions. The simulator is capable of recording real-time data and outputs the information into texts files that are then analyzed in MATLAB. Currently, it is possible to generate the noise of the aircraft as the simulator runs although it is not in real-time.

2.2.1.2. Program Modifications

In order to output the correct data needed for the noise prediction software, some changes had to be made to the current GENHEL-PSU simulation software. The loading for the main rotor was being calculated but not in the frame of reference needed for the noise prediction software. New calculations were implemented in order to get the loadings in the correct blade frame reference (see Appendix B) and then this data was output in the format required by PSU-WOPWOP. The previous version did not have a module that calculated the loading on the auxiliary propeller; therefore a separate module was created using the blade element vortex theorem so that section loading could be calculated on each blade of the auxiliary propeller.

2.3. Acoustic Prediction Model

There has been considerable interest in the prediction of rotor noise ranging from civil aircraft to the military environments. Because of this, there are now numerous ways to predict the noise generated from rotorcraft. They range from methods based upon empirical results to those based upon fundamental governing equations such as the Navier-Stokes (N-S) equation. Today, most of the acoustic prediction methods are based upon the Ffowcs Williams-Hawkings (FW-H) equation, which is an exact rearrangement of the N-S equations and the continuity equation into an inhomogeneous wave equations through the use of generalized functions [**19**] [**20**] [**21**]. In this thesis, the program PSU-WOPWOP is used for all the noise calculations.

2.3.1. PSU-WOPWOP Overview

2.3.1.1. Ffowcs Williams-Hawkings Equation

The origins of aeroacoustic predictions can be traced all the way back to Lighthill's derivation of the acoustic analogy. The main approach is aimed to quantify the strength of the quadrupole source term by comparing how a real fluid and how a uniform acoustic medium at rest behave, both having some sort of fluctuating driving force. A more detailed analysis and the derivation of Lighthill's equation can be viewed in Lighthill's paper, [**22**]. In 1969, Ffowcs Williams and Hawkings published the paper "Sound Generation by Turbulence and Surfaces in Arbitrary Motion," [**23**] which extended Lighthill's acoustic analogy to include the effect of arbitrarily moving surfaces [**22**]. The Ffowcs Williams-Hawkings equation is an exact reformulation of the continuity and Navier-Stokes equation using the theory of generalized functions, which can be written as:

$$\square^2 p'(\vec{x},t) = \frac{\partial}{\partial t}\left\{\left[\rho_0 U_n + \rho\left(u_n - U_n\right)\right]\delta(f)\right\} - \frac{\partial}{\partial x_i}\left\{\left[P_{ij}\hat{n}_j + \rho u_i\left(u_n - U_n\right)\right]\delta(f)\right\} + \frac{\partial^2}{\partial x_i \partial x_j}\left[T_{ij}H(f)\right] \quad (2.1)$$

Here p' is the acoustic pressure, ρ and ρ_0 are the fluid density and density of the undisturbed medium, respectively; u_n and U_n is the normal component of the fluid and integration surface velocities, P_{ij} and T_{ij} are the compressive and Lighthill stress tensors, and $\delta(f)$ and $H(f)$ are the Dirac delta and Heaviside functions, respectively.

The three terms on the right hand side of the FW-H equation are referred to as the monopole, dipole, and quadruple source terms, respectively, due to their mathematical structure. Generalized differentiation is implied in the first two terms due to the presence of the Dirac delta function, $\delta(f)$. Each term in equation (2.1) is a function of f, which is defined as

$$f = \begin{cases} < 0 & \text{Within the data surface} \\ 0 & \text{On the data surface} \\ > 0 & \text{Outside the data surface} \end{cases} \quad (2.2)$$

The monopole and dipole source terms act on the surface where $f = 0$; this is recognized by the presence of the Dirac delta function $\delta(f)$. The quadrupole/volume source term acts in the volume surrounding the surface as indicated by the presence of the Heaviside function which is defined by:

$$H(f) = \begin{cases} 0 & f < 0 \\ 1 & f > 0 \end{cases} \quad (2.3)$$

An integral form of the FW-H equation solution, which neglects the quadrupole term, was developed by Farassat [**24**] and is commonly known as Formulation 1A. This formulation is written as:

$$p'(\boldsymbol{x},t) = p'_T(\boldsymbol{x},t) + p'_L(\boldsymbol{x},t) \qquad (2.4)$$

where the thickness contribution p'_T is

$$4\pi p'_T(\mathbf{x},t) = \int_{f=0}\left[\frac{\rho_0 \dot{U}_n}{r\left|1-M_r\right|^2}\right]_{ret} dS + \int_{f=0}\left[\frac{\rho_0 U_n\left(r\dot{M}_r + cM_r - cM^2\right)}{r^2\left|1-M_r\right|^3}\right]_{ret} dS \qquad (2.5)$$

and the loading contribution is p'_L is

$$4\pi p'_L(\mathbf{x},t) = \frac{1}{c}\int_{f=0}\left[\frac{\dot{L}_r}{r\left|1-M_r\right|^2}\right]_{ret} dS + \int_{f=0}\left[\frac{L_r - L_M}{r^2\left|1-M_r\right|^2}\right]_{ret} dS + \frac{1}{c}\int_{f=0}\left[\frac{L_r\left(r\dot{M}_r + cM_r - cM^2\right)}{r^2\left|1-M_r\right|^3}\right]_{ret} dS \qquad (2.6)$$

Formulation 1A describes the acoustic pressure fluctuation produced by an acoustic data surface (ADS) as a sum of two terms: monopole (thickness) p'_T, and dipole (loading) p'_L; This is shown in equations (2.5) to (2.6). PSU-WOPWOP uses Formulation 1A numerically: integrals are evaluated as discrete sums while derivatives and rates of change are calculated using difference equations. Each term in Formulation 1A is evaluated at the retarded/source time; this is denoted as the subscript *ret* in each integrals. The integrals in the above equations are calculated by summing the contributions of all the sources and nodes on the surface at a particular observer time. Terms with r^{-1} dependency are far-field terms, while terms with r^{-2} dependency are known as near-field terms. Various powers of the Doppler factor, $(1-M_r)^{-1}$, can be found in the denominator of each term of Formulation 1A [**25**].

2.3.1.2. Features

PSU-WOPWOP uses a flexible method for specifying surface and observer motion using objects called ‘changes of base’ (COB). Each COB can specify a single translation, rotation, axis change, or combination of all three. The COB are used together in the code to produce the potentially complex motions of the object being analyzed. The COB required for this thesis are discussed in more detail in Appendix B. The geometry of the integration surfaces is specified by external files called “Patch” files. These contain the definitions of the surfaces in a Plot3D-like format file, which defines each of the blades for each rotor. The blade loads are specified, as input data, on each of the surfaces. For more information on the geometry and loading data and how they were created, see Appendix C. Observer locations can either be specified by a single observer, or by a file that has a grid of observers. Observers can be fixed in space or have their own set of COB allowing them to move arbitrarily. They can also be attached to a specific object, allowing the movement to follow that object. PSU-WOWOP supports many types of frequency analysis, providing functions to calculate SPL, OASPL, and SPL_A as functions of time. PSU-WOPWOP can also calculate OASPL-like quantities over specified frequency ranges.

Three types of surfaces are supported: impermeable surface, compact patches, and permeable surface. Impermeable surfaces are used to represent physical surfaces, such as a rotor blade. A compact patch is similar to the impermeable surface, but it is only a one-dimensional representation of the blade section loads at each spanwise station. Essentially compact patches have already been integrated in the chordwise direction, based on the assumption that the blade is acoustically compact in the chordwise direction. A permeable surface is a fictitious surface placed in the fluid surrounding the rotor blades (or the entire rotor for that matter). Permeable surfaces encompass all physical sources inside the surface, and they are typically used to predict

high-speed impulsive noise, accounting for the quadrupole term of the FW-H equation inside the ADS which otherwise can be very computationally expensive.

2.4. Thesis Configuration Description

The notional compound helicopter used in the analysis is based on the UH-60A helicopter aircraft, but modified such that the main rotor blades have a rectangular plan form and the aircraft includes a wing and an auxiliary propeller for full compounding (see Figure 2-2). These added components provide additional 'control degrees of freedom'. The phrase 'degree of freedom' refers to the number of independent parameters that define a mechanism's ability to move, while the term 'control degrees of freedom' refers to how many ways the pilot is able to control these 'degrees of freedom'. For a conventional helicopter, there are six 'degrees of freedom': up/down, fore/aft, left/right, pitching, rolling, and yawing. These motions are achieved by collectively changing the pitch of the main rotor blades (this will increase thrust), cyclically changing the pitch on the blades (changing the tip path plane), or collectively changing the tail rotor pitch (affecting the yaw moment). The added wing and the auxiliary propeller create new controls that the pilot must handle ('control degrees of freedom'); this means that there are new control inputs to change the six 'degrees of freedom' of the aircraft and trade-offs between all of the mechanisms are now possible.

The specifications are shown in Table 2-1. The main rotor is a four bladed articulated rotor that has collective and cyclic controls. Each blade has feathering, flapping, and lagging motion. A four bladed tail rotor provides the torque to counteract the torque from the main rotor and has collective pitch controls. An added 'control degree of freedom' typically not present on a conventional rotorcraft is the auxiliary propeller. It is located aft of the aircraft and provides the additional thrust required for the aircraft to reach higher forward flight speeds. The auxiliary

propeller model is a seven bladed rotor that has blade pitch controls. All three rotors have variable RPM which allows for each rotor speed to be reduced to a desired amount. All three rotors are on the same drive shaft, so if one rotor's RPM is reduced, the rest follow suit. A wing has also been added on the fuselage to aid in lift as the aircraft reaches higher speeds. As the aircraft reaches critical speeds, this wing will provide lift which tends to offload the main rotor. The wing has control surfaces in the form of flaperons, which provides additional roll control of the aircraft or can be used to vary total lift by deflecting them in the same direction (i.e. use as 'flaps'). Lastly, a stabilator is located near the rear of the aircraft. It is fully controllable and aids in pitch regulation of the aircraft along with stability and trim.

Table 2-1. Notional compound rotorcraft specifications

	Main Rotor	**Tail Rotor**	**Auxiliary Propeller**
Radius (ft)	26.8	5.5	4.0
Chord (ft)	1.73	0.81	0.90
Number of blades	4	4	7
Root twist (deg)	0.0	0.0	83.8
Tip Twist (deg)	-18.0	-17.2	34.6
Omega (rad/s)	27.00	124.62	226.19
Tip Speed (ft/s)	361.56	342.47	452.09
BPF (Hz)	17.2	79.3	252.0
Airfoil	Generic SC Airfoils	NACA 0012	NACA 2412

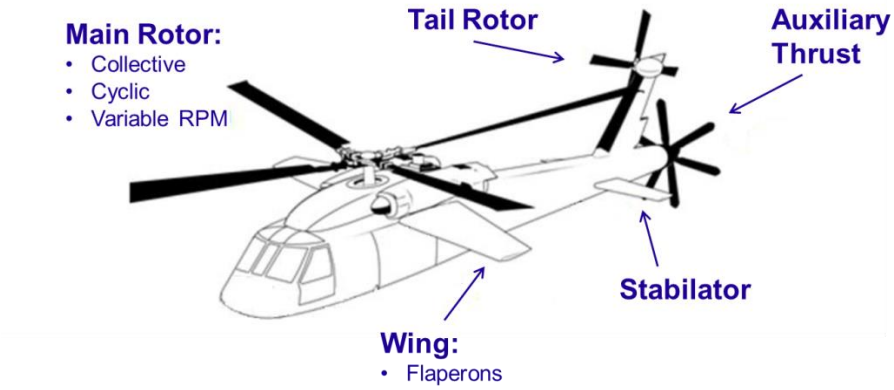

Figure 2-2. Notional compound rotorcraft configuration.

2.5. Approach Details

Although with almost every calculation or experiment, there are approximations and assumptions. The strengths and weaknesses of the current analysis tools will be discussed briefly in the following.

2.5.1. Approach Weaknesses

There are three weaknesses in the current analysis configurations: the software that calculates the loads does not contain a full description of the rotor wake and tip-vortices (the flight simulation software uses a three state Pitt-Peters inflow model [**18**]); the noise prediction software does not calculate high speed impulsive noise; and the chordwise compact loading approximations only produce results of low fidelity noise predictions. The flight simulation software used in this program cannot calculate the blade wake or blade vortex created by the aircraft thus BVI cannot be determined. Blade-vortex interactions where the tip vortex is almost parallel to the rotor blade are one of the most important contributors of noise because they are impulsive and highly directional. When BVI is present, it can dominate the noise spectrum and

be very annoying to human hearing; therefore, it would be beneficial to calculate this term. In the following calculations, it is likely that some of the trim conditions considered resulted in interactions with the tip vortices and the creation of BVI. In this work, the main rotor TPP orientation and the wake skew angle of the air craft and being monitored in-lieu of this weakness. Also, any interaction between the main rotor wake and the tail rotor or auxiliary propeller are being ignored because of this lack of a wake model in the flight simulation software.

The second weakness has to deal with high-speed impulsive noise. At high forward flight speeds, small changes in advancing-tip Mach numbers can result in rapid increases in noise levels and HSI noise can become a major noise source. The noise prediction software used in this analysis is capable of predicting HSI noise if the flow field around the blade is available, but the flight simulation code does not compute the transonic flow field around any of the rotors. Therefore, in this work, HSI noise is ignored, but the advancing-blade tip Mach number, M_{AT}, is being monitored. It is known that if $M_{AT} > 0.85$, the current noise prediction is significantly under predicted ahead and in-plane of the rotor and a more detailed analysis would need to be performed to account for this section of noise.

Finally, an assumption used on the blade loading is a chordwise compact approximation. This means that the loading on all of the blades are represented as a lifting line on the quarter chord of the blade. For the noise prediction software, this approximation means that the loading noise predicted is least accurate in the plane of the rotor. The advantage of having this computation is that the calculations are extremely fast and the required loading information is reasonably accessible. The loading calculated from the flight simulation software is low fidelity, so it is not thought to be a significant factor that the in-plane noise may be incorrect by a few decibels.

2.5.2. Approach Strengths

Even though there are some significant limitations associated with the current noise prediction software, there are some important advantages. Because this study considers the noise of compound rotorcraft in different flight configuration and cases, the vehicle trim is of critical importance. The flight simulation code provides a very good estimate of vehicle trim and provides trade-offs between alternative trim strategies by having a wide variety of user input data. The loads created from the blade-element computations for the main rotor and auxiliary propellers are suitable for low fidelity noise prediction. In the current model, only thickness noise for the tail rotor is being predicted because the loading noise was not readily accessible. Furthermore, the noise prediction code computes the thickness noise and loading noise separately, so the impact of trim on the vehicle rotor noise can be assessed for each noise source independently.

Another feature of the current analysis is that both the flight simulator and chordwise compact blade loading noise computations are extremely fast. There are many trim cases and flight conditions that are being considered in this study, and it is important to be able to do all the calculations quickly. For each case, there are several hundred observer positions used to characterize the noise directivity on a spherical surface surrounding the helicopter. By using parallel computers, these noise computations can be compiled for a complete spherical directivity map in minutes (or tens of minutes).

Chapter 3

Acoustic Prediction Results

3.1. Data Presentation

In order to fully understand the analysis performed in the rest of this thesis, a quick description of the data presentation is now given. One way to show acoustic directivity is to show sound pressure level contours summed over various frequency ranges or bands; this is shown in Figure 3-1. The acoustic measurement locations (otherwise known as the observer locations) for all cases presented are located on a sphere centered on the main rotor hub with a radius of ten main rotor radii (268.373 ft). The observer locations can be described in terms of elevation angle and azimuth angle. The elevation angle is measured above and below the rotor with -90 degrees corresponding below the main rotor, 0 degrees in the plane of the main rotor, and 90 degrees being directly above. The azimuth angle is measured in plane of the main rotor, with 0 and 360 degrees corresponding to the direction of the tail and 180 degrees corresponding to the front of the vehicle (or in the direction of flight). The spherical data is then plotted on a 2-D surface, with the azimuth angle ranging from 360 to 0 degrees. In the right half plot of Figure 3-1, the observer sphere is effectively "unwrapped' such that it is viewed from behind the helicopter. The red center of the rectangular plot corresponds to directly in front and in-plane of the helicopter, where the top edge of the plot matches to the northern pole of the sphere, and the bottom edge matches to the southern pole.

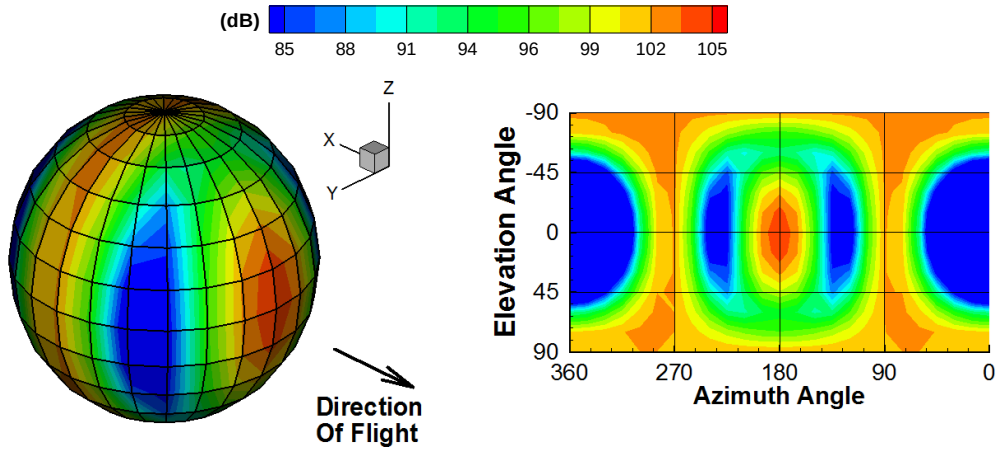

Figure 3-1. Explanation of sound pressure level plots

Figure 3-2 and Figure 3-3 are the acoustic pressure time history plots. They provide another way to understand the directivity of each rotor and how they each contribute to the overall noise of the aircraft. Figure 3-2 shows the acoustic pressure time history at several locations in-plane of the main rotor around the azimuth. The large circle in the middle represents the main rotor, while the two lines near $\psi = 0$ represent the auxiliary propeller and the tail rotor. The direction of flight is in the negative x direction. Figure 3-3 shows the acoustic pressure time history at several locations in a vertical plane that cuts through the centerline of the aircraft, with forward observers to the left and aft observers to the right. The main rotor contributes four large low-frequency pressure pulses directly in front of the aircraft evident in both figures. This is because thickness noise always dominates in the rotor plane. The tail rotor noise can also be seen in the acoustic pressure in front of the helicopter as the smaller amplitude pulses (roughly one half to one third the amplitude of the main rotor pulses) between the large main rotor pulses. The four tail rotor pulses that fall in-between the main rotor have a BPF of about 4.63 times the main rotor and corresponds to the tail rotor thickness noise. The directivity of the auxiliary propeller can be seen in Figure 3-2 at $\psi = 90$ and $\psi = 270$ with the highest frequency pressure pulses occurring. The auxiliary propeller has the highest tip speed and the most blades so the blade

passage frequency (BPF) is much greater than the main rotor and the tail rotor. An examination of Figure 3-3, directly below the rotor, reveals the thickness noise of the auxiliary propeller. Looking at both figures, it can be seen that thickness noise dominates in all regions around the helicopter. This is because there are three rotors all in different orientations producing a wide range of frequencies for thickness noise.

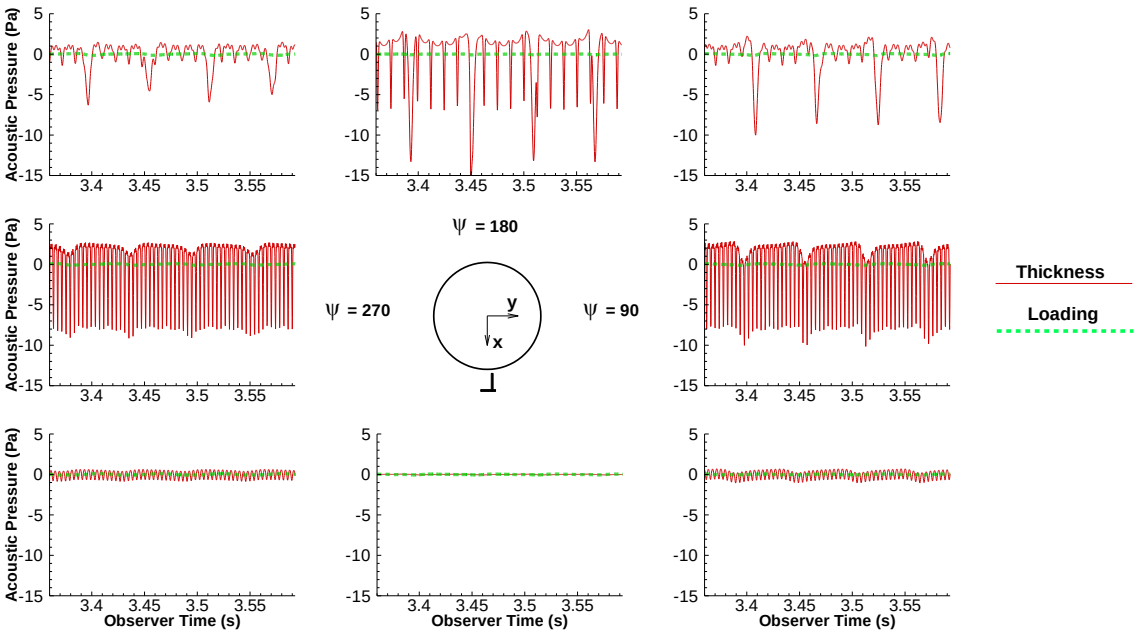

Figure 3-2. Acoustics pressure time history in-plane of the main rotor: 150 knots 100% RPM

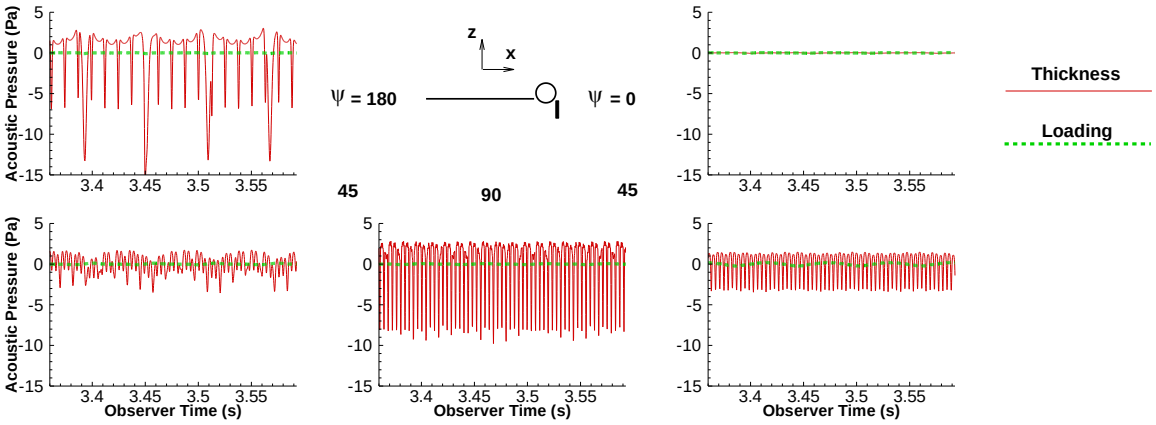

Figure 3-3. Acoustic pressure time history, side view: 150 knots 100% RPM

3.2. Contributions from Each Rotor

As discussed in the introduction, the aircraft being analyzed has extra ‘control degrees of freedom’ including a horizontal wing and an auxiliary propeller located aft on the aircraft. Both of these devices are used to trim the vehicle. It is important to understand the noise generated from each rotor located on the helicopter. Note that only rotor discrete frequency noise is being considered in the following calculations. Each rotor has been separately analyzed in order to understand the directivity produced and to see how they combine to provide the total acoustic field observed around the aircraft.

Figure 3-4 shows the total noise (including thickness and loading) sound pressure level plots for three frequency bands for each of the rotors on the compound rotorcraft. The low frequency band ranges from 0 Hz – 70 Hz; the middle frequency band ranges from 70 Hz – 245 Hz; and the high frequency band ranges from 245 Hz – 1000 Hz. The top row in Figure 3-4 shows the computations for the main rotor (BPF = 17.5 Hz); the second row shows noise computations for the tail rotor (BPF = 79 Hz); the third show shows noise computations for the auxiliary propeller (BPF = 252 Hz); and the bottom show shows the noise predictions when all three rotors and included.

It can be seen that the main rotor noise primarily contributes to the low frequency band with the directivity in front and in-plane of the main rotor. This corresponds to the thickness noise always dominating in-plane of every rotor. The tail rotor noise dominates the middle frequency band, once again radiating in front and in-plane of the tail rotor. The tail rotor can be heard at the poles of the aircraft because it is oriented 90 degrees from the main rotor plane; this shifts the thickness noise directivity. The auxiliary propeller dominates the highest frequency band; dominating everywhere out of the plan of the main rotor. The auxiliary propeller has the highest SPL and is in the highest frequency range so it would be most annoying to human hearing. The

reason it has the highest noise is due to its high tip Mach number; resulting in high thickness noise.

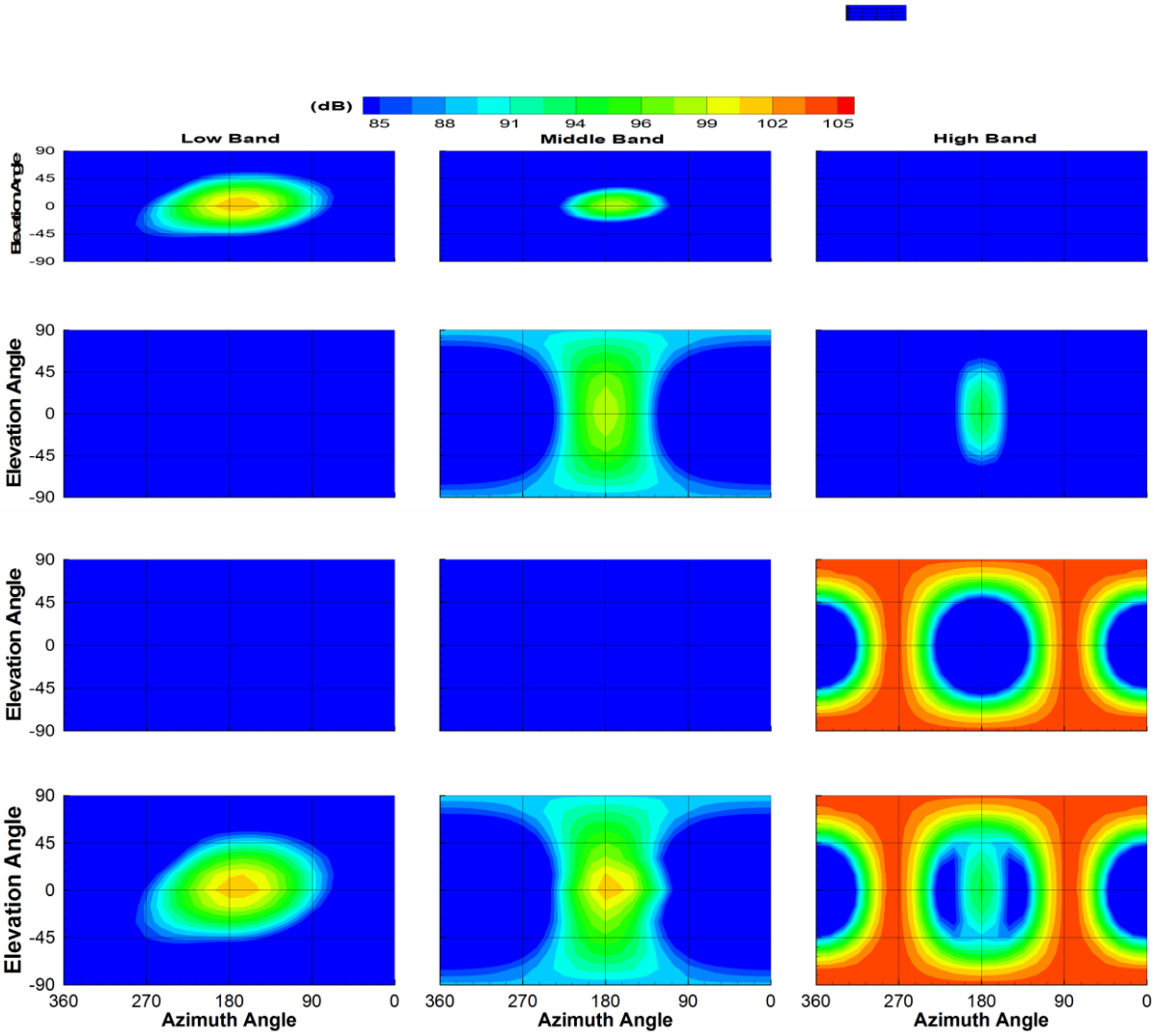

Figure 3-4. Comparison of noise from configuration components. Top row: main rotor; 2nd row: tail rotor; 3rd row: auxiliary propeller; bottom row: total noise from all rotors

3.3. Variation in Performance

A major advantage of having a compound helicopter is that there are multiple ways to achieve trim at each flight condition. For example, propulsive force can be traded off between

the auxiliary propeller and the main rotor or the lifting force can be exchanged between the wing and the main rotor. These extra 'control degrees of freedom' can be used to optimize the trim for different cases and can potentially lead to different noise levels and directivity radiated from each rotor. In the following sections, various trim combinations will be explored in the context of the impact each has on the total rotor noise of the compound rotorcraft. The variations that were investigated were flight speed, rotor tip speed, auxiliary propeller thrust and auxiliary propeller tip speed. As each case was varied, the other components of the aircraft were adjusted accordingly to ensure proper vehicle trim. These results from the trim states were then analyzed from the acoustic viewpoint.

3.2.1. Forward Flight Speed Variation

One of the most important advantages of having a compound rotorcraft is the ability for the vehicle to fly at higher speeds. Conventional helicopters have problems with high speed flight because the power required and vibrations increases. Conventional helicopters cannot reach the same speeds compound rotorcraft can because of the high advancing tip Mach numbers produced by the main rotor at the higher speeds. The loading required by the main rotor to maintain these high speeds are not achievable, this is because the retreating side of the rotor would result in blade stall and the advancing side would have transonic flow and increased drag. With the addition of the wing, the main rotor is now offloaded and with the addition of the auxiliary propeller, a sufficient amount of thrust is now available to achieve fast forward flight.

The noise of a helicopter in high-speed flight increases rapidly as the transonic flow on the advancing blade results in high-speed impulsive noise. Generally, HSI noise should be avoided due to the impulsive nature and high noise levels. HSI noise is closely associated with the appearance of shocks and transonic flow around the advancing rotor blades. These appear in

the high speed flight cases. With the current simulation program, GENHEL-PSU, speeds any higher that 200 knots result in inaccurate aerodynamic loads, therefore they will not be investigated. Once again, PSU-WOPWOP noise predictions are under predicted because the program does not compute HSI noise, but the changes in thickness noise are still useful and can provide some understanding of how compound rotorcraft can benefit acoustically from high-speed flight.

In order to understand what happens to the acoustics of a compound rotorcraft when only the flight speed is changed, some cases have been studied and are show in Table 3-1, for a more detailed analysis on the wing and the auxiliary propeller see Appendix A. The first case is described in column one: 150 knot forward flight speed, with 100% all rotor RPM resulting in a main rotor advancing tip Mach number of 0.876. The second case, show in column 2 has a forward flight speed of 200 knots and all rotors are operation at 100% RPM. The second case is possible because the auxiliary propeller takes the main role of producing the propulsive force. It is obvious that the noise of the higher speed case should be much louder (especially the thickness noise) because of the very high advancing tip Mach number reaching 0.951.

Table 3-1. Case information

	150 kts	200 kts	200 kts
Main Rotor			
% RPM	100	100	88.4
M_{AT}	0.876	0.951	0.876
TPP Angle (deg)	8.68	12.44	11.62
Propulsive Force (lbs)	1100.0	340.0	-190.0
Lifting Force (lbs)	14350.0	11800.0	8330.0
Aux Prop			
% RPM	100	100	88.4
M_{AT}	0.842	0.865	0.776
Propulsive Force (lbs)	570.0	2700.0	3010.0
Wing			
Lifting Force (lbs)	5840.0	9420.0	12550.0

Figure 3-5 shows the difference in the SPL's between the two cases: 150 knots is on the top row and 200 knot case is the middle row (both with 100% RPM for all rotors). The low, middle, and high frequency band levels are shown here for the full configuration of the aircraft (this includes all three rotors). Notice that in the 200 knot, 100% RPM case, additional noise is produced, reaching levels up to 118 dB. This is because the main rotor's advancing tip Mach number is greater than 0.95, thus creating large pressure pulses. This can be confirmed by looking at the region in-plane and ahead of the main rotor on the low frequency plot of the 200 knot, 100% case. The directionality matches that created by the thickness noise. This follows suit with the middle band representing the tail rotor, and the highest band representing the auxiliary propeller. Overall, an increase in the flight speed results in a large increase in noise for this case.

It should be noted, that the 200 knot, 100% RPM case is not realistic because the HSI noise would likely be as high as or higher than the thickness noise in the plane of the rotor at this flight condition. Therefore, it is reasonable to assume that at this advancing tip Mach number, the peak noise is underestimated by 50% or more. Also note, that in the flight simulation software, the trim window the program successfully ran is very small, this means that the flight condition is very unstable. In reality, it would be very difficult for the pilot to maintain control of this aircraft at this configuration.

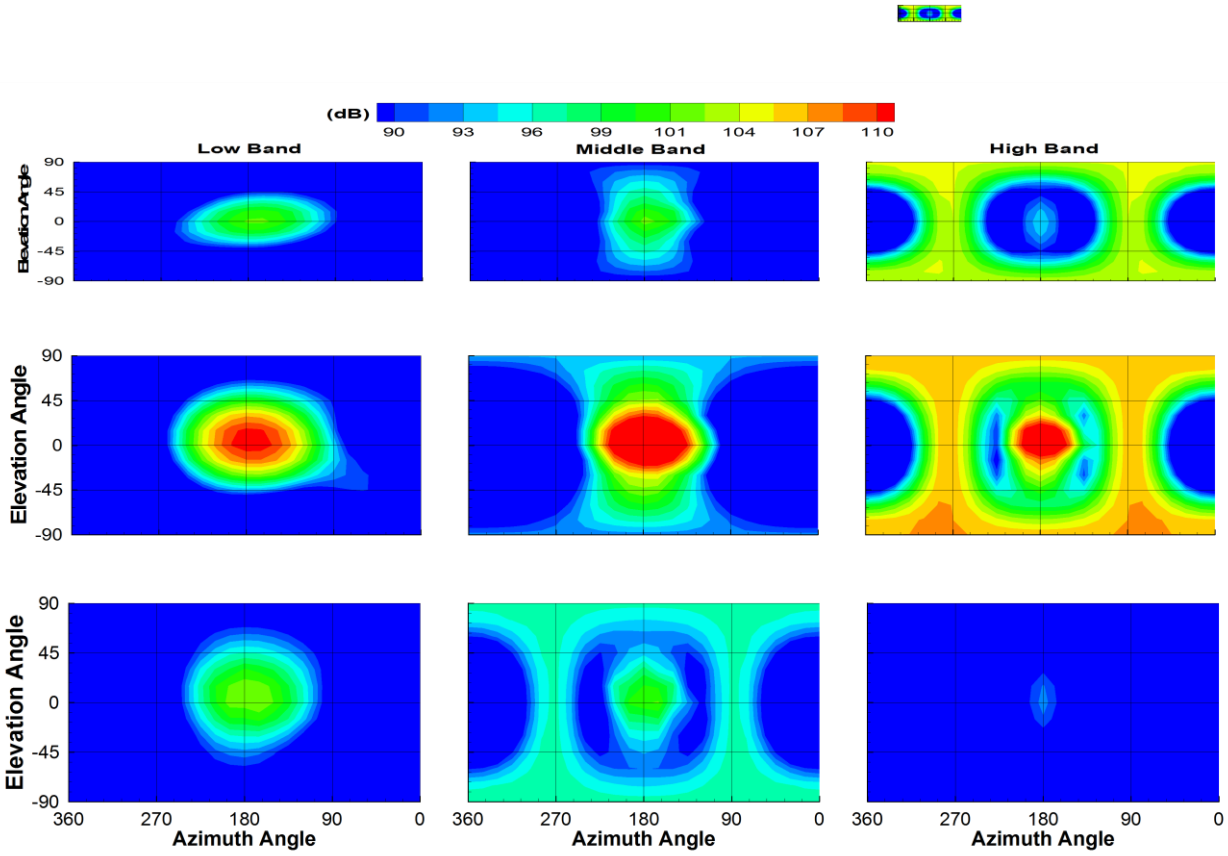

Figure 3-5. Forward flight speed variation. Top row: 150 knots 100% RPM; Middle row: 200 knots 100% RPM; Bottom row: 200 knots 88.4% RPM

3.2.2. Rotor RPM Variation

The most direct way to reduce rotor noise is to reduce the advancing-tip Mach number of the rotor. This will lower the thickness noise in-plane of the rotor, which is the dominate noise source in high-speed flight. Note: thickness noise and high speed impulsive noise are both important in high-speed forward flight, but they have similar directivity: in-plane and forward of the rotorcraft. Both of these are strongly impacted by the advancing tip Mach number. With a compound configuration, it is possible to consider changing all rotor RPM while simultaneously changing the speed in which the helicopter flies. It would be most interesting to match flight cases depending on advancing tip Mach numbers and then accurately analyze the noise. In the previous section, the tip speeds of each rotor were not reduced for the highest speed case. This resulted in large increases in noise ahead and in-plane of the rotor and made trimming the aircraft difficult for a single auxiliary propeller setting.

Referring back to Table 3-1, the third column has yet to be discussed but is now relevant in this consideration of varying rotor RPM. This last column shows a case of 200 knots with all rotors operating at 88.4% RPM. This RPM was selected such that the advancing tip Mach number of the main rotor for the 200 knot flight speed matches the 150 knot case considered previously. The RPM reduction occurs for all of the rotors simultaneously because they are share the same drive shaft in the simulation model. Table 3-1 shows the key parameters of the two flight speed cases and their respective trim. Looking at the thrust on the higher speed and lower RPM case, the auxiliary propeller creates so much propulsive force that the main rotor begins to create drag. This is due to the main rotor achieving a ‘blow back’ scenario where its only use is to control the aircraft and provide some lift.

Once again, with the approximations in both the simulation program and the noise prediction software, BVI and intense HSI noise can be prevalent but are not calculated. In lieu of

this, the tip path plane (TPP) angles along with the wake skew angles are being monitored and shown in Table 3-1. A TPP is the imaginary circular plane outlined by the rotor blade tips in making a cycle of rotation, while the TPP angle is the angle between the imaginary circle and the oncoming flow. The small TPP for the 150 knot case suggests that possible blade vortex interaction may occur in this trim condition, but a higher fidelity analysis is needed to determine whether or not BVI noise would actually occur.

The bottom row in Figure 3-5 shows the SPL's for each frequency band for the 200 knot 88.4% RPM case. Examination of the lowest frequency plot reveals that the levels have dropped drastically compared to the 200 knot 100% case. This lowest frequency plot corresponds to the main rotor and its directivity can be seen in-plane and in front of the aircraft. Comparing the third row to the first row (which is the 150 knot and 100% RPM), the levels are almost identical. This is because their advancing tip Mach numbers have been matched on purpose in order to see if a better flight condition with lower/same noise is possible. This trend transfers over to the tail rotor. In the second column, the middle band corresponds to the tail rotor. With its reduction in RPM, it now matches the 150 knot and 100% RPM case in noise level and directivity. Looking at the highest frequency band (third column), it can be seen that not much noise is being shown at those higher frequencies. This highest frequency band corresponds to the auxiliary propeller on our previous cases. The reason there is no contribution in this band is because with the reduction of RPM's of every rotor, the BPF of the auxiliary propeller has now dropped to the middle band. This proves that with the reduction in RPM, a large noise reduction can be achieved even on the most dominate noise source.

The in-plane acoustic pressure time histories for the 150 knot, 200 knot, and reduced RPM 200 knot case are shown in Figure 3-2, Figure 3-6, and Figure 3-7 respectively. Note in the 200 knot 100% RPM case in Figure 3-6, the acoustic pressure levels are much higher than the other two. This is because when the aircraft operates at 100% RPM, the advancing tip Mach

number is so large that large fluctuations in the noise occurs and shocks start to form. This is primarily due to the thickness noise. If HSI noise was calculated, the acoustic pressure would have a much higher amplitude and would be very impulsive. Notice in Figure 3-7 there are fewer acoustic pressure pulses compared to Figure 3-2. This is a direct result of reducing all rotor RPM's. Comparing Figure 3-2 and Figure 3-7, notice that with the reduction of the RPM, the two figures look very similar in amplitude around the entire azimuth. This is because the advancing tip Mach numbers have been chosen to be the same through the reduced rotation speed in the 88.4% RPM case (200 knots). This data shows that it is possible to fly a compound rotorcraft at higher speeds with a reduction in noise and with little to no performance penalty.

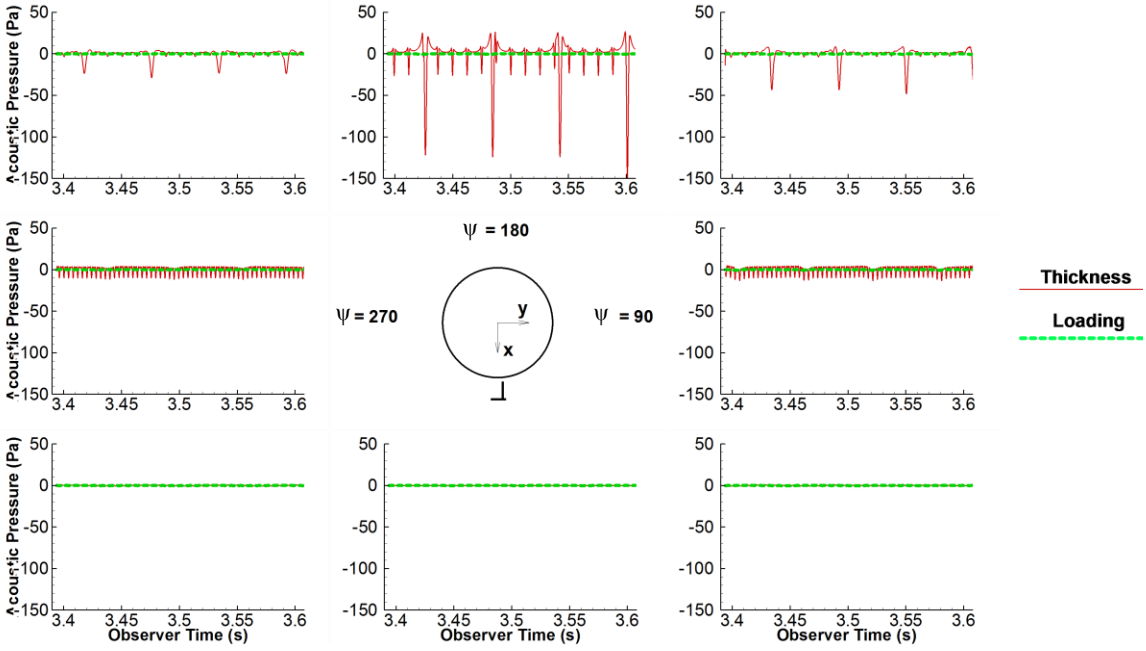

Figure 3-6. Acoustic pressure time history, in plane of the main rotor: 200 knots 100% RPM

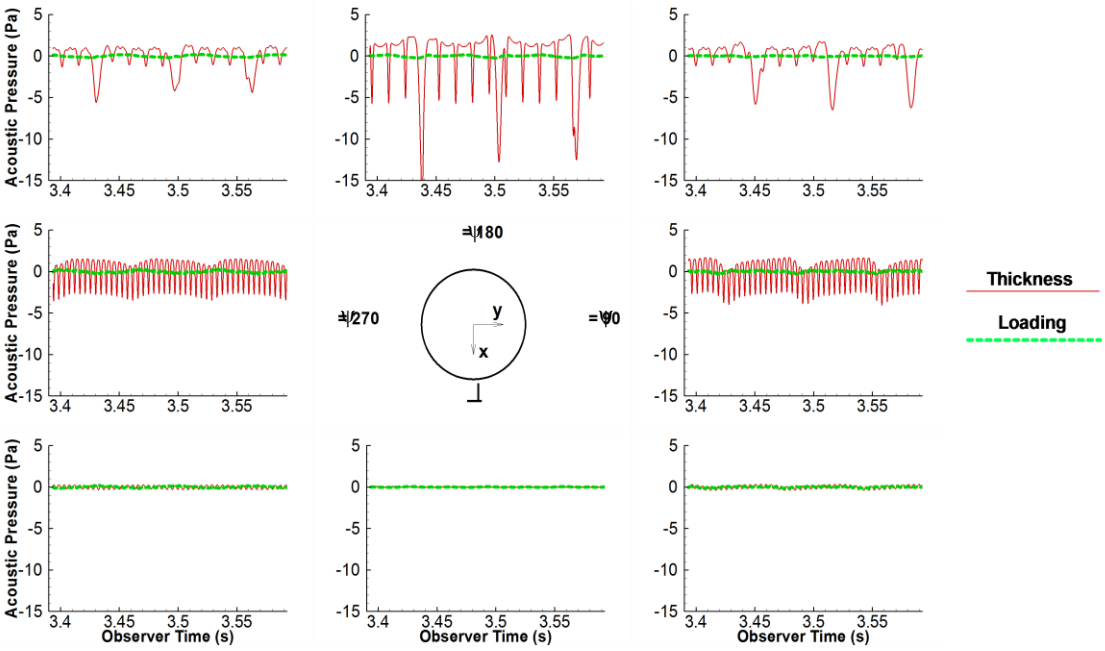

Figure 3-7. Acoustic pressure time history, in plane of the main rotor: 200 knots 88.4% RPM

3.2.3. Auxiliary Propeller Thrust Variation

A key feature of the notional compound helicopter is the auxiliary propeller and its ability to provide additional propulsive thrust so higher flight speeds can be reached. In particular, the auxiliary propeller enables the 200 knot forward flight speed while the main rotor RPM is reduced. Increasing the thrust produced by the auxiliary propeller results in an offloading of the main rotor. This is because the main rotor no longer needs to produce as much forward force as it is being provided by the auxiliary propeller. This change will affect the TPP angle of the main rotor, the directivity of the main rotor thickness noise, and the loading noise produced by the main rotor. Table 3-2 shows the forces produced as the auxiliary propeller thrust is increased. As more thrust is produced by the auxiliary propeller, the wing starts to act as the primary lifting mechanism. Similarly, the main rotor propulsive force is reduced as the auxiliary propeller thrust increases because the auxiliary propeller is now the main provider of forward thrust.

Table 3-2. Auxiliary propeller thrust variation

Aux Prop Propulsive Force (lbs)	Main Rotor Propulsive Force (lbs)	Main Rotor Lifting Force (lbs)	Wing Lifting Force (lbs)	Tip Path Plane Angle (deg)
150 knots (100% RPM)				
560.0	1090.0	14350.0	5840.0	8.68
1400.0	250.0	11670.0	8220.0	6.41
2100.0	-450.0	7450.0	11200.0	2.68
200 knots (88.4% RPM)				
3010.0	-190.0	8330.0	12540.0	11.62
3360.0	-540.0	6110.0	14490.0	9.93
3710.0	-890.0	2900.0	17280.0	6.78

Figure 3-8 shows the SPL of the high frequency band for just the loading noise on the auxiliary propeller as the auxiliary propeller thrust is varied for the same cases showed in Table 3-2. Note that the dB scale is lower than the previous figures, ranging from about 50-75 dB. This figure demonstrates that as auxiliary propeller thrust is increased, the loading noise from the auxiliary propeller also increases. Although comparing this to Figure 3-9, which is high frequency of the full configuration (all rotors), it can be seen that for the same thrust variations as before, there is not much (if any) change in the total noise. This is because thickness noise is the dominant noise source for this aircraft regardless of observer location. So even though loading changes are evident, they do not add significantly to thickness noise in this flight conditions.

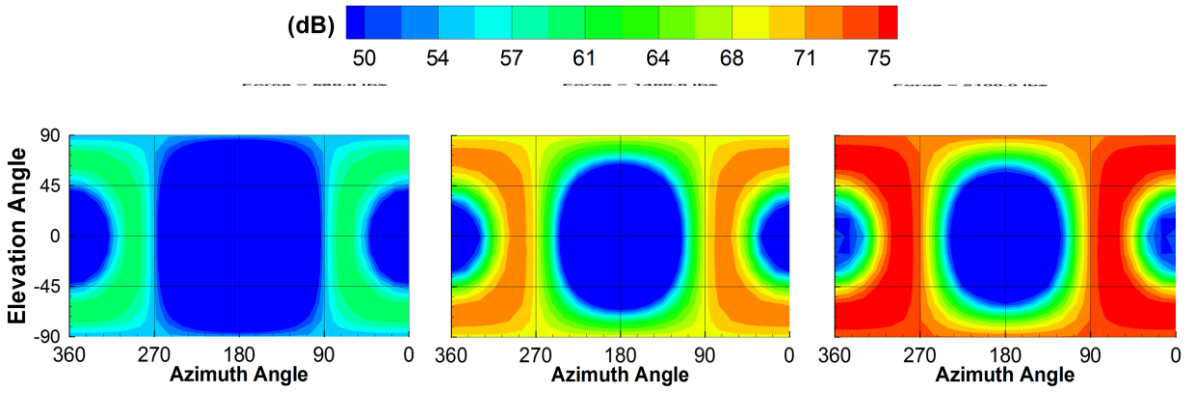

Figure 3-8. Auxiliary propeller thrust variation. 150 knots 100% rotor RPM; Auxiliary propeller loading noise only; SPL in the highest frequency band.

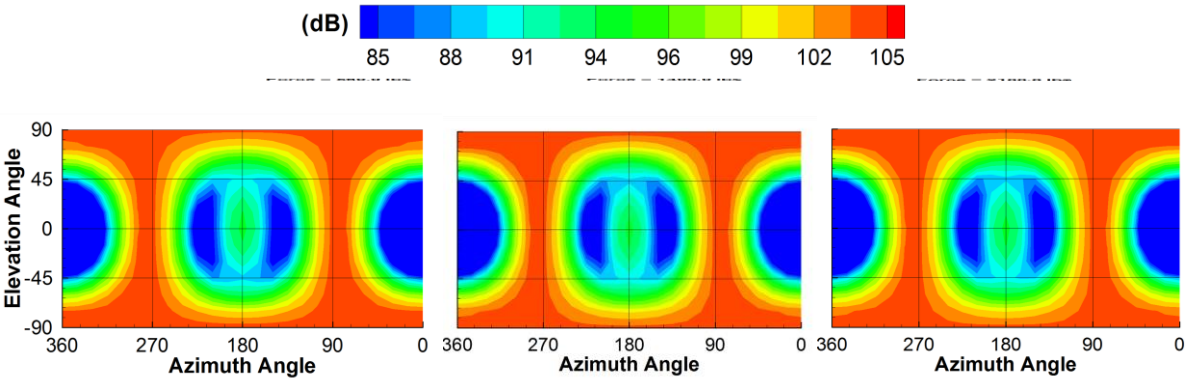

Figure 3-9. Auxiliary propeller thrust variation. 150 knots 100% rotor RPM; Noise from all rotors; SPL in the highest frequency band.

3.2.4. Auxiliary Propeller Tip Speed Variation

In the previous analysis, the dominant noise was the thickness noise of the auxiliary propeller. It had the highest amplitude over the largest region of the spherical observer surface. This is a result of a high tip Mach number of the auxiliary propeller and the orientation of the propeller as compared to the other two rotors. Since the auxiliary propeller creates the highest noise, it would be advantageous to lower the auxiliary propeller tip speed as much as possible

while still maintaining the same performance. The auxiliary propeller operates in the highest frequency band which is most annoying to human hearing and its directivity is primarily below the aircraft. When in-plane noise is important, the aircraft is normally far down range when ground based observers hear the main rotor in-plane noise, but as the vehicle flies overheard, the noise directed downward from the auxiliary propeller is most important – and much closer. This downward directivity could cause some annoyance in populated areas to civilians so it would be beneficial to reduce it as much as possible.

To reduce the rotor tip speed, the RPM must be reduced. It is possible in this model to independently reduce the auxiliary propeller without affecting the main rotor and tail rotor. Instead of using a ratio as done in previous RPM reductions, this new technique is done by setting the original value of the auxiliary propeller to a lower number. The overall sound pressure level (OASPL or 0-1000 Hz in this case) is shown in Figure 3-10 for three different auxiliary propeller speeds: 100%, 95%, and 90%. The top row is the noise from all the rotors and the bottom row is just the noise from the auxiliary propeller. Looking at both plots, as the auxiliary propeller's RPM is reduced the overall noise is decreased dramatically. This is because the advancing tip Mach number is decreasing thus reducing the thickness noise contributions.

A major advantage to reducing the tip Mach number of just the auxiliary propeller independently is that it is no longer the dominant noise source. Examining the top row in Figure 3-10, on the 90% plot, the highest amplitude noise is now in-plane in front of the rotor. This space corresponds to the main rotor and tail rotor thickness noise. The areas in which the auxiliary propeller previously dominated have been reduced by about 8-10 dB which is significant. It would now be possible to change the aircraft configuration if a low noise flight is required. For example, the helicopter could fly at full 100% RPM, this would be loud, but it may provide better performance. Then, if a low noise configuration is required, the auxiliary propeller

could be reduced to 90% while maintaining forward flight speed. This would make the aircraft less annoying to the population.

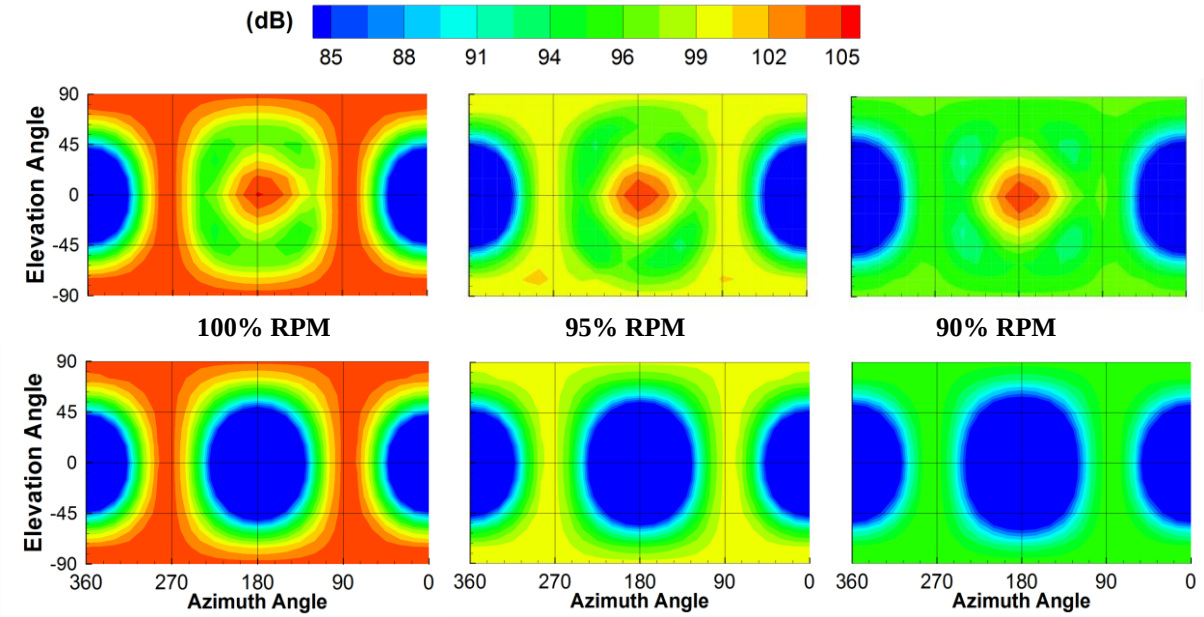

Figure 3-10. Overall SPL (0-1000 Hz) for auxiliary propeller at various RPM settings. Top: noise from all rotors, Bottom: auxiliary propeller thickness noise only.

Chapter 4

Summary and Future Work

4.1. Summary and Conclusions

From these preliminary results, it is clear that substantial changes to helicopter rotor noise can be reached through trade-offs between the extra ‘control degrees of freedom’ available in a compound rotorcraft. Particularly, it was shown that a reduction in all rotor advancing-tip Mach numbers had a dramatic impact on the overall noise levels. This was because thickness noise was the dominate noise source in each case investigated, and as tip speed is reduced, so is thickness noise. This data showed that it is possible to fly a compound rotorcraft at higher speeds with a reduction in noise with little to no performance penalties. In addition to reducing noise at a particular forward velocity, it was also found that a reduction of rotor tip speeds combined with auxiliary lift from the wing and auxiliary propulsive from the propeller enabled the aircraft to fly faster with less noise. Results showed that auxiliary propeller thrust changes led to very small changes in the overall noise levels and small changes in the TPP angles. It was evident that loading noise does increase as auxiliary propeller thrust increases and it can affect performance of the aircraft, but thickness noise levels are drastically higher than loading so there are no changes to overall sound pressure. Changing the auxiliary propeller tip speed independently of the other rotors resulted in very large noise reduction, especially at high forward flight speeds. The greatest noise reductions were found to be out of plane of the main rotor. Results showed that for the greatest noise reduction, the auxiliary propeller tip speed should be reduced as much as possible. However through testing, for this specific configuration, a reduction in the auxiliary propeller tip speed did not affect he performance of the vehicle drastically.

4.2. Future Work and Possible Improvements

In order to figure out which configuration and flight condition would be best with respect to noise, there are a few ways to classify what is desired. One way is to look at an integrated noise metric or single sound pressure level. This could be done by integrating the data over the entire sphere and taking an average (i.e. essentially giving a sound power level). An investigation of the lowest noise cases would reveal exactly which case is the overall lowest.

Another way to classify which configuration is best would be to consider the mission requirements. A customer might want a specific frequency range which is important to minimize noise. This type of analysis is possible with these tools. Since each rotor contributes specifically to its own frequency band, the analysis of lowering a specific range is available. Similarly, the customer might want the noise reduced in a specific region on the ground (a specific directivity). For example, if the customer wanted the noise below the rotor to stay as low as possible, plots and figures could be used from this analysis to determine if the aircraft has reached the clients standards.

References

[1] J. Seddon and Simon Newman, *Basic Helicopter Aerodynamics Second Edition*. Reston, VA: AIAA Education Series, 2001.

[2] Simon Newman, "The Compound Helicopter Configuration and the Helicopter," *Aircraft Engineering and Aerospace Technology*, vol. 69, no. 5, pp. 407-413, 1997.

[3] Brian Geiger, Flight control optimization on a fully compounded helicopter with redundant control effectors, 2005.

[4] J. Gordon Leishman, *Principles of Helicopter Aerodynamics*. New York: Cambridge University Press, 2008.

[5] M Orchard and S Newman, "The Fundamental Configuration and design of the compound helicopter," *Proceedings of the Institution of Mechanical Engineers Part G Journal of Aerospace Engineering*, vol. 217, pp. 297-315, December 2003.

[6] Art Linden. (2013, April) S-69 (XH-59A) Advancing Blade Concept Demonstrator. [Online]. http://www.sikorskyarchives.com/S-69%20%28XH-59A%29.php

[7] Kenneth S. Brentner and F. Farassat, "Modeling aerodynamically generated sound of helicopter rotors," *Progress in Aerospace Sciences 39*, pp. 83-120, 2003.

[8] Wayne Johnson, "Noise," in *Helicopter Theory*. New York: Dover Publications, 1980, pp. 903-957.

[9] K.S. Brentner and F. Farassat, "Helicopter Noise Prediction: The Current Status and Future Direction," *Journal of Sound and Vibration*, vol. 170, no. 1, pp. 79-96, 1994.

[10] Thomas F. Brooks and Casey L. Burley, "Rotor broadband noise prediction with comparison to model data," 2001.

[11] D.A. Conner, B.D. Edwards, W.A. Decker, M.A. Marcolini, and P.D. Klein, "NASA/ARMY/Bell XV-15 Tiltrotor Low Noise Terminal Area Operations Flight Research program," in *Paper AIAA 2000-1923, 6th AIAA/CEAS Aeroacoustics Conference*, Lahaina, Hawaii, June 12-14, 2000.

[12] David A. Conner and J. Brent Wellman, "Hover Acoustic Characteristics of the XV-15 with Advanced Technology Blade," *Journal of Aircraft*, vol. 31, no. 4, pp. 737-744, Aug. 1994.

[13] Martin D. Maisel, Demo J. Giulianetti, and Daniel C. Dugan, The History of the XV-15 Tilt Rotor Aircaft From Concept to Flight, 2000.

[14] United States. National Aeronautical and Space Administartion. Scientific and Technical Information Office., "Quiet, powered-lift propulsion: A converence held at Lewis Research Center.," Cleveland, Ohio, November 14-15, 1978.

[15] Carl Russell and Wayne Johnson, "Conceptual Design and Performance Analysis for a Large Civil Compound Helicopter," in *AHS Future Vertical Lift Aircraft Design Converence*, San Franciso, CA, January 18-20.

[16] J. Howlett, UH-60A BLACK HAWK Engineering Simulation Program: Volume I - Mathematical Model, 1981.

[17] Taha Ozdemir and Joseph, F. Horn, "Simulation Analysis of Flight Control Law with In-Flight Optimization," *American Helicopter Society Forum 68th Annual Proceedings, Ft. Worth, TX*, May 2013.

[18] Wayne Johnson, *Rotorcraft Aeromechanics*. Cambridge: Cambridge University Press, 2013.

[19] G. A. Brès, Modeling the noise of arbitrary maneuvering rotorcraft: analysis and implementation of the PSU-WOPWOP noise preduction code, June 2002.

[20] G. Perez, Investigation of the influence of maneuver of rotorcraft noise, June 2002.

[21] G.A. Brès, K.S. Brentner, G. Perez, and H.E. Jones, "Maneuvering rotorcraft noise prediction," *Journal of Soun and Vibration*, vol. 275(3-5), pp. 719-738, August 2004.

[22] M.J. Lighthill, "On Sound Generated Aerodynamically, I: General Theory," *Proceedings of the Royal Society*, vol. A211, pp. 564-587, 1952.

[23] J.E. Ffowcs Williams and David L. Hawkings, "Sound Generated by Turbulence and Surfaces in Arbitrary Motion," *Philosophical Transactions of the Royal Society*, vol. A264, no. 1151, pp. 321-342, 1969.

[24] F. Farassat and G.P. Succi, "The Prediction of Helicopter Discrete Frequency Noise," *Vertica*, vol. 7, no. 4, pp. 309-320, 1983.

[25] Benjamin Goldman, Modifications to PSU-WOPWOP for Enhanced Noise Prediction Capabilities, 2012.

Appendix A

Lift and Force comparisons

Figure A-1 represents a graphical view of Table 3-1. The three main cases that are being compared are shown on the y-axis. The reason for the 200 knot, 88.4% case was to have the same advancing tip Mach number as the 150 knot, 100% RPM case. Looking at the left plot, the lifting force of the main rotor and the wing are plotted against each other. As the aircraft achieves greater forward flight speed and/or reduces the rotor RPM, the wing starts to take over the majority of the lifting load. This trade-off is necessary for the aircraft to achieve and maintain these higher speeds. The plot on the right shows the propulsive force balance between the main rotor and the auxiliary propeller. As the aircraft reaches higher forward speeds and/or reduced rotor RPM, it is necessary for the auxiliary propeller to generate the main portion of the propulsive force. It is noted in the 200 knot, 88.4% RPM case, the main rotor acts as a drag force. This is because the oncoming flow creates a blow-back phenomenon and creates more drag than lift. In practice this should be avoided.

Figure A-1. Lift and propulsive force comparisons.

Appendix B

Coordinate Transformations

PSU-WOPWOP uses changes of base to position each component of the aircraft in the proper position and to describe the motion of the aircraft and its components. Each blade starts out in a global reference axes. In order for each rotor to be in its correct space and for each blade to mimic the correct flapping and lagging, COB are defined by the user through of coordinate transformations. The user inputs translations, rotations, or axis changes in the namelist file. For this thesis, the following coordinate transformations are used to represent the GENHEL-PSU model as closely as possible. The aircraft starts out in a global frame of reference (0,0,0) which corresponds to the center of gravity of the aircraft. The first step is to place the main rotor hub to its correct location in space, Figure B-1 shows this translation. This type of translation is also necessary for the tail rotor and the auxiliary propeller. The next COB encompasses the shaft tilt rotation of the main rotor; this is shown in Figure B-2. Only the main rotor has tilt in this model. Figure B-3 shows how each main rotor blade is rotated around the +Z axis. Each blade has to be offset to its correct azimuth angle with blade one being at $\psi = 0$, blade two at $\psi = 90$, etc. The following translation is the hinge offset, e; this is done on the Y axis. Next the aircraft inputs the lead/lag on the blade with positive lag in the +Y axes with variable representation δ. Next, the flapping of the blade is input, with positive flap in the +Z axes with variable representation β. For this notional aircraft, the components are positioned in a manner similar to that described in the UH-60A BLACK HAWK Engineering Simulation Program: Volume 1 – Mathematical Model, [**16**].

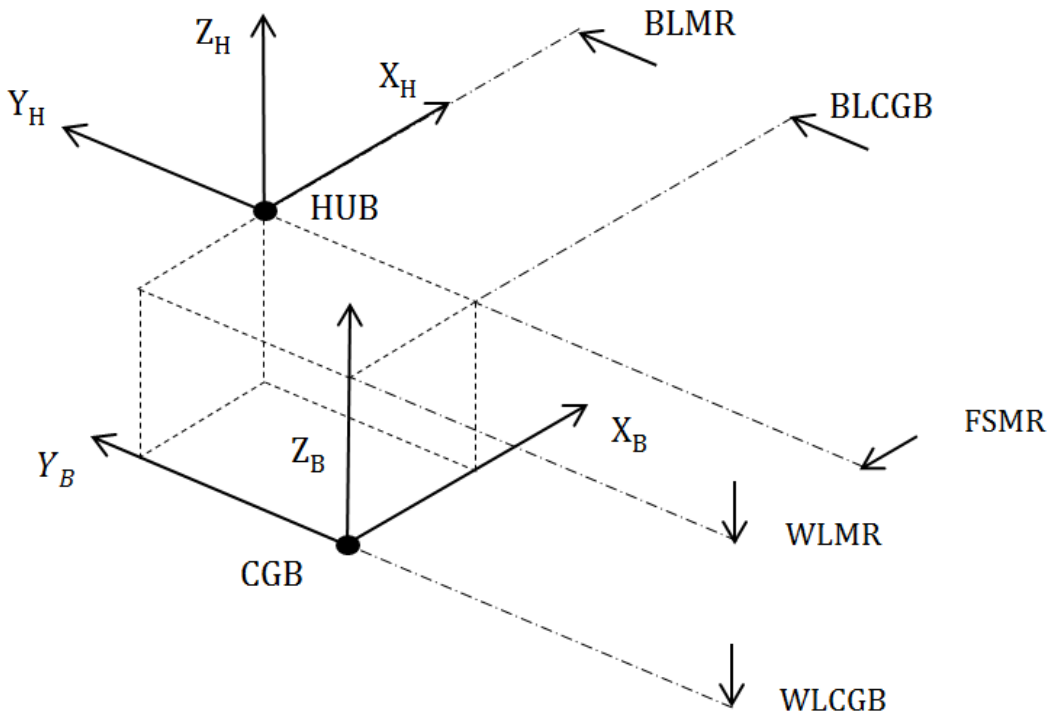

Figure B-1. Body Axis to Hub Axes Transformation

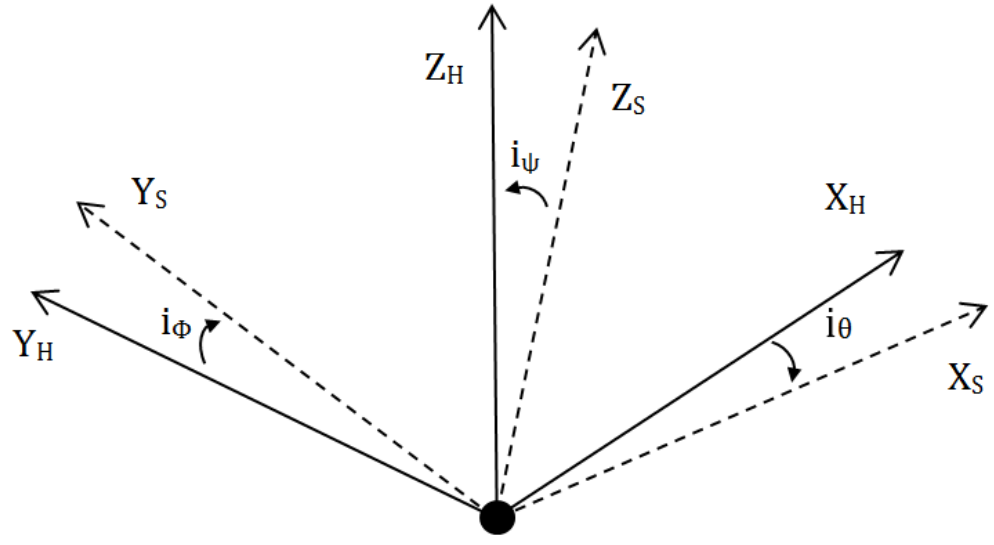

Figure B-2. Hub Axis to Shaft Axes Transformation

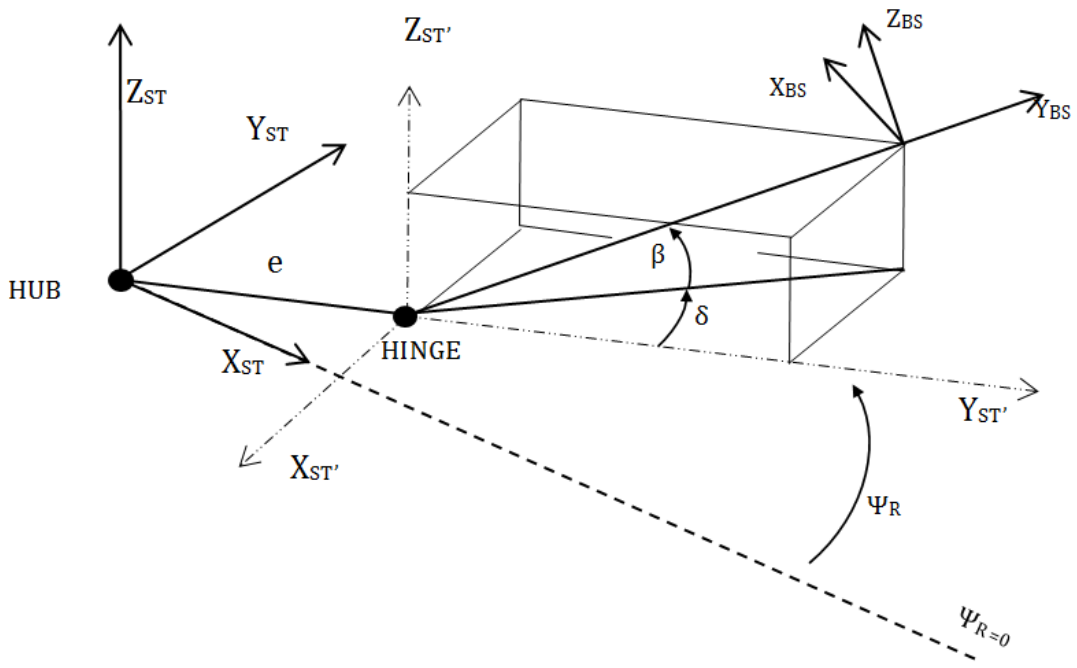

Figure B-3. +Z Coordinate Axes to Rotating Blade Span Axes Transformation

Appendix C

Blade Maker

BladeMaker is a program that creates a blade object by taking blade definitions at different span wise locations on a rotor blade. Taper, sweep, offset, flex, twist, and airfoil curve make the blade geometry. All of these parameters are needed at only those span locations where there is change. Previous to the research done in this thesis, BladeMaker was only able to create blades with any NACA 4 or 5 digit series airfoil. A feature was added to use the best fit line equations so additional airfoils could be used.

BladeMaker blade geometry files can be used in other codes, such as PSU-WOPWOP for computing various geometric parameters. Specifically, PSU-WOPWOP needs a thickness patch in order to create the thickness noise for the helicopter. Patch files are binary files and can be written in either big-endian or little-endian format. Top views of each rotor are shown below in

the figures below; the parameters of each blade are shown in the tables below. Note that the main rotor and tail rotor have constant chords and linear twist.

Figure C-1. Main rotor top view plan form (not to scale)

Figure C-2. Auxiliary propeller top view plan form (not to scale)

Figure C-3. Tail rotor top view plan form (not to scale)

Table C-1. Main rotor and tail rotor specifications

	Main Rotor	**Tail Rotor**
c/R	0.065	0.147
Tip Twist [°]	-18	-17.2
t/c	0.091	0.120

Table C-2. Auxiliary propeller specifications

r/R	c/R	Pitch	t/c
[-]	[-]	[°]	[-]
0.00	Spinner	-	Spinner
0.05	Spinner	-	Spinner
0.10	0.019	83.8	0.122
0.15	0.040	79.3	0.121
0.20	0.066	75.0	0.122
0.25	0.094	70.9	0.122
0.30	0.123	67.0	0.122
0.35	0.149	63.4	0.122
0.40	0.172	60.0	0.121
0.45	0.191	56.8	0.122
0.50	0.207	53.9	0.121
0.55	0.218	51.2	0.122
0.60	0.224	48.7	0.122
0.65	0.227	46.4	0.122
0.70	0.226	44.3	0.121
0.75	0.219	42.4	0.121
0.80	0.208	40.6	0.122
0.85	0.190	38.9	0.121
0.90	0.164	37.4	0.122
0.95	0.121	35.9	0.122
1.00	0.006	34.6	0.122

Appendix D

GENHEL-PSU Code

Following is the module that is in the code GENHEL-PSU. This module takes the blade loading data generated from GENHEL-PSU and converts it into a binary file that PSU-WOPWOP requires.

```
MODULE WOPWOPCONVERTER
    IMPLICIT NONE

        integer:: MagicNumber, MajorVersion, MinorVersion, GeomFile,
        Structured, Unstructured, Constant, Periodic
        integer:: Aperiodic, FuncFile, NodeCenteredNormals,
        FaceCentered, Zero, SurfacePressure, SurfaceLoadingVector
        integer:: FlowParameters, RefGroundFixed, RefRotatingGround,
        RefPatchFixed, SingPrecision, DoubPrecision, NumSteps
        integer:: FloatingPoint, numzones, zone1, zone2, zone3, zone4,
        iMax1, jMax1, fulltime
        integer:: part1, part2, int0, kk, bladefileno,totaldata,
        totaldata2, bladeno, hh, length, length2
        integer:: iout,nlines,n, nlines2, imax_p, jmax_p
        integer:: first, last, AUXnBladeSeg
        real:: stepsize, fpfirst, fplast, ftfirst, ftlast, timestep,
        step, newnSimStep, rootcutout, MyTimeStep
        real:: SPAR, OFFSET, R_p, AUX_seg_length
        character:: Comment1*1024,Comment2*32, c, my_unit*20,
        Comment3*32
        real,dimension(:),allocatable:: force_fp, force_ft, force_fr,
        zerosz, lagangle, flapangle, AP_force_drag, AP_force_lift
        real,dimension(:),allocatable:: dD_p, dL_p,AUX_zerosz_long
        real,dimension(19):: AUX_zerosz

        INTEGER,PARAMETER :: nSegMax=50
        DOUBLE PRECISION:: DELSEG(nSegMax), SEGOUT(nSegMax),
SEGIN(nSegMax)

        COMMON /WOPWOP/ SPAR, OFFSET
        COMMON /WOPWOP2/ DELSEG, SEGOUT, SEGIN


    CONTAINS

    SUBROUTINE FORCE

        USE model, ONLY: RMR
        USE SimData, ONLY: iCurrStep
        Use RotorData, ONLY: nBladeSeg, nBlade
```

```
        Use ControllerData, ONLY: SimTime


        ! CONVERT TO STD UNITS (m,N,Pa)
        RMR = RMR*0.3048
        MyTimeStep = .005

        !Radius of aux prop
        R_p = 1.2192 !m
        AUXnBladeSeg = 19


        ! Open data from GENHEL files
        open(unit = 99, file='../Commands/command.txt')
        open(unit = 100, file = 'FP_data.dat',status='OLD')
        open(unit = 200, file = 'FT_data.dat',status='OLD')
        open(unit = 300, file = 'FR_data.dat',status='OLD')
        open(unit = 198,  file = 'Drag.dat',status = 'OLD')
        open(unit = 197,  file = 'Lift.dat',status = 'OLD')

        ! initialize then read in size of force data
        totaldata = 0
        totaldata2 = 0

        !Main rotor
        DO
           read(100,*,end=10)nlines
           totaldata = totaldata+1
        END DO
     10 rewind(100) !close then reopen

        !Aux prop
        DO
           read(198,*,end=11)nlines2
           totaldata2 = totaldata2+1
        END DO
     11 rewind(198)

        read(99,*) newnSimStep !fulltime read in

        !main rotor
        iout = 10
        DO n=1,nBlade
           write(my_unit,"(a,i1.1)") "forces_blade",n
           open(unit = iout, status = 'replace', file =
'..\BIN\outputs\'//trim(my_unit)//'.dat', form = 'binary')
           iout = iout+1
        END DO

        !Aux prop
        open(unit = 1001, status = 'replace', file =
'..\BIN\outputs\PropLoading.dat', form = 'binary')

        MagicNumber = 42
        MajorVersion = 1
```

```
MinorVersion = 0
GeomFile = 1
Structured = 1
Unstructured = 2
Constant = 1
Periodic = 2
Aperiodic = 3
FuncFile = 2
NodeCenteredNormals = 1
FaceCentered = 2
Zero = 0
SurfacePressure = 1
SurfaceLoadingVector = 2
FlowParameters = 3
RefGroundFixed = 1
RefRotatingGround = 2
RefPatchFixed = 3
SingPrecision = 1
DoubPrecision = 2
FloatingPoint = 1
numzones = 1
zone1 = 1
zone2 = 2
zone3 = 3
zone4 = 4
Comment1="This file contains loading information"
Comment2="Blade"
Comment3="Aux Prop Loading"
iMax1 = 10
jMax1 = 1
imax_p = 19
jmax_p = 1


allocate(force_fp(totaldata))
allocate(force_ft(totaldata))
allocate(force_fr(totaldata))
allocate(zerosz(nBladeSeg))
allocate(AP_force_drag(totaldata2))
allocate(AP_force_lift(totaldata2))
allocate(dD_p(totaldata2))
allocate(dL_p(totaldata2))
allocate(AUX_zerosz_long(totaldata2))

! read in all the data of force
DO part1 = 1,totaldata
   read(100,*) force_fp(part1)
   read(200,*) force_ft(part1)
   read(300,*) force_fr(part1)
END DO

DO part2 = 1,totaldata2
   read(198,*) dD_p(part2)
   read(197,*) dL_p(part2)
END DO
```

```
! create zeros
DO int0 = 1,nBladeSeg
   zerosz(int0) = 0
END DO

DO int0 = 1, AuxnBladeSeg
   AUX_zerosz(int0) = 0
END DO


length = 1 + SimTime/MyTimeStep ! extra 1 is for zero

DO int0 = 1, totaldata2
   AUX_zerosz_long(int0) = 0
END DO

iout = 10
DO hh = 1,nBlade
   write(iout) MagicNumber
   write(iout) MajorVersion
   write(iout) MinorVersion
   write(iout) Comment1
   write(iout) FuncFile
   write(iout) numzones
   write(iout) Structured
   write(iout) Aperiodic
   write(iout) NodeCenteredNormals
   write(iout) SurfaceLoadingVector
   write(iout) RefPatchFixed
   write(iout) FloatingPoint
   write(iout) Zero
   write(iout) Zero
   write(iout) numzones
   write(iout) zone1
   write(iout) Comment2
   write(iout) (length-13000)
   write(iout) iMax1
   write(iout) jMax1

   iout = iout + 1
END DO

!write to aux prop loading files
write(1001) MagicNumber
write(1001) MajorVersion
write(1001) MinorVersion
write(1001) Comment1
write(1001) FuncFile
write(1001) numzones
write(1001) Structured
write(1001) Constant
write(1001) NodeCenteredNormals
write(1001) SurfaceLoadingVector
write(1001) RefPatchFixed
```

```
          write(1001) FloatingPoint
          write(1001) Zero
          write(1001) Zero
          write(1001) numzones
          write(1001) zone1
          write(1001) Comment3
          !write(1001) (length-13000)
          write(1001) imax_p
          write(1001) jmax_p

          !just for initialization
          timestep = 0
          step = 0

          ! Write out data for main rotor
          DO kk = 1,length
             iout = 10
             DO n = 1,nBlade
                first = (1+(n-1)*nBladeSeg+step)
                last = first + nBladeSeg -1
                ! dont forget conversion 14.593902936 converts it to
lb*ft to N*m
                if (timestep .gt. 65) then
                  write(iout) (timestep-65)
                  write(iout) 1.35581795*force_fr(first:last)
                  write(iout) 1.35581795*force_ft(first:last)
                  write(iout) -1.35581795*force_fp(first:last)
                else
                continue
                end if
                iout = iout+1
             END DO

             step = nbladeseg*nBlade + step
             timestep = timestep + MyTimeStep

          END DO

          timestep = 0
          first = 0
          last = 0
          step = 0
          ! Write out data for AUX prop
          DO kk = 1,length
             first = 1+step
             last =  first + (AUXnBladeSeg-1)
             if (timestep.gt.65) then
               write(1001) 1.35581795*dD_P(first:last)
               write(1001) AUX_zerosz_long(first:last)
               write(1001) 1.35581795*dL_p(first:last)
               GO TO 100
             end if

             timestep = timestep+MyTimeStep
             step = AUXnBladeSeg + step
```

```
        END DO


   100  close(10)
        close(11)
        close(12)
        close(13)
        close(14)
        close(15)

        close(197)
        close(198)
        close(1001)
      END SUBROUTINE

      SUBROUTINE GEOMETRY
         USE model, ONLY: RMR
         Use RotorData, ONLY: nBladeSeg, nBlade, nSegmax

         integer:: onezone, int0, intone, int1, AUXnBladeSeg, imax_p,
jmax_p
         real:: segment, AUX_segment, span_seg_old
         real,dimension(:),allocatable:: span_seg_new, zeros, ones,
zeros_sweep
         real,dimension(19):: AUX_span_seg, AUX_zeros, AUX_ones,
AUX_span_seg_old, AUX_span_center
         real,dimension(19):: AUX_span_center_old
         character:: units*32,Comment1*1024, patch1*32, patch2*32
         MyTimeStep = .005

         open(unit = 111, status= 'replace', file =
'..\BIN\outputs\PropGeometry.dat', form = 'binary')
         open(unit = 11, status='replace',
file='..\BIN\outputs\geometry_converter.dat', form = 'binary')
         units = "lb/ft^2"
         patch1 = "Blade 1"
         patch2 = "Auxprop"
         Comment1= "This file contains geometry information"

         allocate(span_seg_new(nBladeSeg))
         allocate(zeros(nBladeSeg))
         allocate(ones(nBladeSeg))
         allocate(zeros_Sweep(nBladeSeg))
         onezone = 1
         imax_p = 19
         jmax_p = 1
         AuxnBladeSeg = 19


         write(11) MagicNumber
         write(11) MajorVersion
         write(11) MinorVersion
         write(11) units
         write(11) Comment1
```

```
write(11) GeomFile
write(11) onezone
write(11) Structured
write(11) Constant
write(11) NodeCenteredNormals
write(11) FloatingPoint
write(11) Zero
write(11) Zero
write(11) patch1
write(11) iMax1
write(11) jMax1

write(111) MagicNumber
write(111) MajorVersion
write(111) MinorVersion
write(111) units
write(111) Comment1
write(111) GeomFile
write(111) onezone
write(111) Structured
write(111) Constant
write(111) NodeCenteredNormals
write(111) FloatingPoint
write(111) Zero
write(111) Zero
write(111) patch2
write(111) iMax_p
write(111) jMax_p


rootcutout = (OFFSET+SPAR)*0.3048
segment = 0
AUX_segment = 0
span_seg_old = 0
AUX_span_seg_old = 0
span_seg_new = 0
AUX_span_seg = 0

! Create array of zeroes
DO int0 = 1,nBladeSeg
   zeros(int0) = 0
END DO

DO int0 = 1,AUXnBladeSeg
   AUX_zeros(int0) = 0
END DO

! Create array of ones
DO intone = 1,nBladeSeg
   ones(intone) = 1 !changes from 0 to 1
END DO

DO intone = 1, AUXnBladeSeg
   AUX_ones(intone) = 1
END DO
```

```
        DO int1 = 1,nBladeSeg
           span_seg_new(int1) =
(((SEGOUT(int1)*RMR)+(SEGIN(int1)*RMR))/2)-
(((SEGOUT(1)*RMR)+(SEGIN(1)*RMR))/2)
           span_seg_old = span_seg_new(int1)
        END DO

        AUX_seg_length = 0
        AUX_span_seg_old = 0.12192
        !AUX_span_seg(1) = 0.12192

        DO int1 = 1, AUXnBladeSeg
           AUX_span_seg(int1) = AUX_span_seg_old(int1) + AUX_seg_length
           AUX_seg_length = (R_p - .12192)/(AUXnBladeSeg-1)
           AUX_span_seg_old = AUX_span_seg(int1)
        END DO

        zeros_sweep = zeros
        zeros_sweep(10) = .21078244

        ! Write geometry coordinates (rotations will occur inside
WOPWOP) ^+y --> +x
        write(11) zeros !x
        write(11) span_seg_new !y
        write(11) zeros !z

        ! Write out normal coordinates (required for WOPWOP but zeros
because it is a compact patch)
        write(11) zeros
        write(11) zeros
        write(11) ones

        !write prop geometry
        write(111) AUX_zeros
        write(111) AUX_span_seg
        write(111) AUX_zeros

        !write out normal coordinates for prop
        write(111) AUX_zeros
        write(111) AUX_zeros
        write(111) AUX_ones


        CLOSE(11)
        CLOSE(111)
     END SUBROUTINE

     SUBROUTINE ANGLES
        Use ControllerData, ONLY: SimTime
        Use RotorData, ONLY: nBladeSeg, nBlade

        INTEGER:: ANGLEFLAG, TRANSLATIONFLAG, AXISFLAG, I, iout1,
iout2, H, m, new_length
        INTEGER:: COB1, COB2
```

```
        REAL:: time
        CHARACTER:: my_unit1*30, my_unit2*30

        MyTimeStep = .005 !add my own stuff

        ANGLEFLAG = 1
        TRANSLATIONFLAG = 0
        AXISFLAG = 0
        COB1 = 1
        COB2 = 2

        OPEN(unit = 1, status = 'old', file = 'Flapping_Angles.dat')
        OPEN(unit = 2, status = 'old', file = 'Lagging_Angles.dat')

        iout1 = (10+nBlade)
        iout2 = (iout+nBlade)
        DO n=1,nBlade
           write(my_unit1,"(a,i1.1)") "Flapping_Angles_WOPWOP",n
           write(my_unit2,"(a,i1.1)") "Lagging_Angles_WOPWOP",n
           open(unit = iout1, status = 'replace', file =
'..\BIN\outputs\'//trim(my_unit1)//'.dat')!, form = 'binary')
           open(unit = iout2, status = 'replace', file =
'..\BIN\outputs\'//trim(my_unit2)//'.dat')!, form = 'binary')
           iout1 = iout1+1
           iout2 = iout2+1
        END DO

        new_length = length-13000
        allocate(lagangle(length*nBlade))
        allocate(flapangle(length*nBlade))

        ! read in all the data of force
        DO part1 = 1,(length*nBlade)
           read(1,*) flapangle(part1)
           read(2,*) lagangle(part1)
        END DO

        iout1 = (10+nBlade)
        iout2 = (iout+nBlade)


        DO n = 1, nBlade
           write(iout1,*) COB1
           write(iout2,*) COB2
           write(iout1,*) new_length
           write(iout2,*) new_length
           write(iout1,*) ANGLEFLAG, TRANSLATIONFLAG, AXISFLAG
           write(iout2,*) ANGLEFLAG, TRANSLATIONFLAG, AXISFLAG

           time = 0
           DO I = 1, length
              if (I .gt. 13000) then
                write(iout1,*) (time-65.00391)
                write(iout2,*) (time-65.00391)
              else
```

```
            continue
          end if
          time = time + MyTimeStep

       END DO


       iout1 = iout1 + 1
       iout2 = iout2 + 1
    END DO

    iout1 = (10+nBlade)
    iout2 = (iout+nBlade)

    DO m = 1, nBlade
       H = 1*m
       step = 0
       DO n = 1, length
          if (n .gt. 13000) then
            write(iout1,*) flapangle(H+step)
            write(iout2,*) -lagangle(H+step)
          else
            continue
          end if
          step = step + nBlade
       END DO
       iout1 = iout1 + 1
       iout2 = iout2 + 1
    END DO

  END SUBROUTINE ANGLES

END MODULE WOPWOPConverter
```

Appendix E

PSU-WOPWOP Namelist File

The following is the Namelist file PSU-WOPWOP requires to generate the noise data. This file shows all of the changes of base that are discussed in Appendix B. For a better upstanding of each function, please refer to the PSU-WOPWOP user manual.

```
&EnvironmentIn

  nbObserverContainers = 1
  nbSourceContainers = 1
  !sigmaFlag=.true.
  !sigmaFolderName   ='/'
  ASCIIOutputFlag=.true.
  SPLFolderName     ='/'
  debugLevel = 1
  OASPLdBFlag = .true.
  OASPLdBAFlag = .true.
  SPLdBFlag = .true.
  SPLdBAFlag = .true.
  spectrumFlag = .true.

  thicknessNoiseFlag=.true.
  acousticpressureflag = .true.
  loadingnoiseflag = .true.
  totalnoiseflag = .true.

  !loadingSigmaflag = .true.
  !machSigmaFlag = .true.
  !normalSigmaFlag = .true.
  !thicknessnoisesigmaflag = .true.
  !observersigmaflag = .true.

/

&EnvironmentConstants
  rho= 1.225
  c = 340 !m/s
/
&ObserverIn

  nt = 256
```

```
  octaveflag = .true.
  octavenumber = 3
  octaveApproxFlag=.true.

  !sperical observer grid
  radius = 81.8 !m
  nbTheta = 9
  nbPsi = 7
  thetamin = 0
  thetamax = 6.28318531
  psimin = -1.57079633  !-90
  psimax = 1.57079633  !90



  nbBase = 1
  windowFunction='Hanning Window'
  lowPassFrequency=1260.
  highPassFrequency=1.

/

&CB
  Title = 'Shaft tilt for observer'
  axisType='TimeIndependent'
  axisValue=0.0,1.0,0.0
  angletype = 'timeindependent'
  anglevalue = .0523599
/


&CB
  Title = 'observer translation'
  translationType='KnownFunction'
  VH = -102.889,0.0,0.0 !m/s
/
&ContainerIn
  Title='Compund Configuration 1 BLAH'
  nbContainer=2
  ntau = 256
  taumin = 3.0
  taumax = 3.45
  !dTau = .00517 !every 8 deg (MR) , matches genhel
/
&ContainerIn
  Title='Main Rotor'
  nbContainer=2
  nbBase= 2
```

```
  ! dtau = .00517
/

&CB
   translationType='KnownFunction'
   VH = -102.889,0.0,0.0 !m/s
/
&CB
   Title="Angular Rotation"
   AngleType="KnownFunction"
   Omega=  24.3  !rad/s
   axisType='TimeIndependent'
   AxisValue=0.0,0.0,1.0
   psi0 = -1.57079633
/
&ContainerIn
   Title = 'Thickness Files'
   nbcontainer = 4
   nbBase = 0

/

 &ContainerIn
   Title='Blade 1 Thickness'
   patchGeometryFile='OUTPUTS/outSTD.wop'
   nbBase=6

/
 &CB
   Title='Offset for blade 1'
   axisType='TimeIndependent'
   axisValue=0.0,0.0,1.0
   angleType='TimeIndependent'
   angleValue =0.0
/
&CB
   Title = 'offset pitching axis to 1/4 chord'
   translationvalue = .131826,0.,0.
/
&CB
   Title = 'Hinge Offset'
   translationtype = 'timeindependent'
   translationvalue =0.0,.381,0.0
/

 &CB
   Title = 'Lead Lag Blade 1'
   iB = 2
   AngleType = 'nonperiodic'
```

```
  filename = '/OUTPUTS/Lagging_Angles_WOPWOP1.dat'
  Axistype = 'timeindependent'
  Axisvalue = 0.,0.,1.
/
 &CB
  Title = 'Flapping Blade 1'
  iB = 1
  Axistype = 'timeindependent'
  Axisvalue = 1.,0.,0.
  AngleType = 'nonperiodic'
  filename = '/OUTPUTS/Flapping_Angles_WOPWOP1.dat'


/
 &CB
  Title = 'Spar Offset Final'
  Translationtype = 'timeindependent'
  translationvalue = 0.,.6858,0.

/

 &ContainerIn
  Title='Blade 2 Thickness'
  patchGeometryFile='OUTPUTS/outSTD.wop'
  nbBase=6

/
 &CB
  Title='Offset for blade 2'
  axisType='TimeIndependent'
  axisValue=0.0,0.0,1.0
  angleType='TimeIndependent'
  angleValue =1.57079633
/
&CB
  Title = 'offset pitching axis to 1/4 chord'
  translationvalue = .131826,0.,0.
/
&CB
  Title = 'Hinge Offset'
  translationtype = 'timeindependent'
  translationvalue =0.0,.381,0.0
/

 &CB
  Title = 'Lead Lag Blade 2'
  iB = 2
  AngleType = 'nonperiodic'
  filename = '/OUTPUTS/Lagging_Angles_WOPWOP2.dat'
```

```
  Axistype = 'timeindependent'
  Axisvalue = 0.,0.,1.
/
 &CB
  Title = 'Flapping Blade 2'
  iB = 1
  Axistype = 'timeindependent'
  Axisvalue = 1.,0.,0.
  AngleType = 'nonperiodic'
  filename = '/OUTPUTS/Flapping_Angles_WOPWOP2.dat'


/
 &CB
  Title = 'Spar Offset Final'
  Translationtype = 'timeindependent'
  translationvalue = 0.,.6858,0.

/

 &ContainerIn
  Title='Blade 3 Thickness'
  patchGeometryFile='OUTPUTS/outSTD.wop'
  nbBase=6
/
 &CB
  Title='Offset for blade 3'
  axisType='TimeIndependent'
  axisValue=0.0,0.0,1.0
  angleType='TimeIndependent'
  angleValue =3.14159265
/
&CB
  Title = 'offset pitching axis to 1/4 chord'
  translationvalue = .131826,0.,0.
/
&CB
  Title = 'Hinge Offset'
  translationtype = 'timeindependent'
  translationvalue =0.0,.381,0.0
/

 &CB
  Title = 'Lead Lag Blade 3'
  iB = 2
  AngleType = 'nonperiodic'
  filename = '/OUTPUTS/Lagging_Angles_WOPWOP3.dat'
  Axistype = 'timeindependent'
  Axisvalue = 0.,0.,1.
```

```
/
 &CB
   Title = 'Flapping Blade 3'
   iB = 1
   Axistype = 'timeindependent'
   Axisvalue = 1.,0.,0.
   AngleType = 'nonperiodic'
   filename = '/OUTPUTS/Flapping_Angles_WOPWOP3.dat'


/
 &CB
   Title = 'Spar Offset Final'
   Translationtype = 'timeindependent'
   translationvalue = 0.,.6858,0.
/
 &ContainerIn
   Title='Blade 4 Thickness'
   patchGeometryFile='OUTPUTS/outSTD.wop'
   nbBase=6
/
 &CB
   Title='Offset for blade 4'
   axisType='TimeIndependent'
   axisValue=0.0,0.0,1.0
   angleType='TimeIndependent'
   angleValue =4.71238898
/
&CB
   Title = 'offset pitching axis to 1/4 chord'
   translationvalue = .131826,0.,0.

 /
&CB
   Title = 'Hinge Offset'
   translationtype = 'timeindependent'
   translationvalue =0.0,.381,0.0
/

 &CB
   Title = 'Lead Lag Blade 4'
   iB = 2
   AngleType = 'nonperiodic'
   filename = '/OUTPUTS/Lagging_Angles_WOPWOP4.dat'
   Axistype = 'timeindependent'
   Axisvalue = 0.,0.,1.
/
 &CB
   Title = 'Flapping Blade 4'
```

```
  iB = 1
  Axistype = 'timeindependent'
  Axisvalue = 1.,0.,0.
  AngleType = 'nonperiodic'
  filename = '/OUTPUTS/Flapping_Angles_WOPWOP4.dat'


/
 &CB
  Title = 'Spar Offset Final'
  Translationtype = 'timeindependent'
  translationvalue = 0.,.6858,0.

/
&ContainerIn
  Title = 'Loading Files'
  nbcontainer =4
  nbBase = 0

/


&ContainerIn
  Title='Blade 1 Loading'
  patchGeometryFile='OUTPUTS/geometry_converter.dat'
  patchLoadingFile='OUTPUTS/forces_blade1.dat'
  nbBase=5
/
&CB
  Title='Offset for blade 1 (0 Degrees)'
  axisType='TimeIndependent'
  axisValue=0.0,0.0,1.0
  angleType='TimeIndependent'
  angleValue =0
/
&CB
  Title = 'Hinge Offset'
  translationtype = 'timeindependent'
  translationvalue =0.0,.381,0.0
/

 &CB
  Title = 'Lead Lag Blade 1'
  iB = 2
  AngleType = 'nonperiodic'
  filename = '/OUTPUTS/Lagging_Angles_WOPWOP1.dat'
  Axistype = 'timeindependent'
  Axisvalue = 0.,0.,1.
/
```

```
 &CB
   Title = 'Flapping Blade 1'
   iB = 1
   Axistype = 'timeindependent'
   Axisvalue = 1.,0.,0.
   AngleType = 'nonperiodic'
   filename = '/OUTPUTS/Flapping_Angles_WOPWOP1.dat'

/
 &CB
   Title = 'Spar offset final'
   translationtype = 'timeindependent'
   translationvalue = 0.0,1.54091278,0.
/


&ContainerIn
   Title='Blade 2 Loading'
   patchGeometryFile='OUTPUTS/geometry_converter.dat'
   patchLoadingFile='OUTPUTS/forces_blade2.dat'
   nbBase=5
/

&CB
   Title='Offset for blade 2 (90 Degrees)'
   axisType='TimeIndependent'
   axisValue=0.0,0.0,1.0
   angleType='TimeIndependent'
   angleValue =1.57079633
/
&CB
   Title = 'Hinge Offset'
   translationtype = 'timeindependent'
   translationvalue =0.0,.381,0.0
/
 &CB
   Title = 'Lead Lag Blade 2'
   iB = 2
   AngleType = 'nonperiodic'
   filename = '/OUTPUTS/Lagging_Angles_WOPWOP2.dat'
   Axistype = 'timeindependent'
   Axisvalue = 0.,0.,1.
/
 &CB
   Title = 'Flapping Blade 2'
   iB = 1
   Axistype = 'timeindependent'
   Axisvalue = 1.,0.,0.
   AngleType = 'nonperiodic'
```

```
  filename = '/OUTPUTS/Flapping_Angles_WOPWOP2.dat'

/
 &CB
  Title = 'Spar offset final'
  translationtype = 'timeindependent'
  translationvalue = 0.0,1.54091278,0.
/

&ContainerIn
  Title='Blade 3 Loading'
  patchGeometryFile='OUTPUTS/geometry_converter.dat'
  patchLoadingFile='OUTPUTS/forces_blade3.dat'
  nbBase=5

/

&CB
  Title='Offset for blade 3 (180 Degrees)'
  axisType='TimeIndependent'
  axisValue=0.0,0.0,1.0
  angleType='TimeIndependent'
  angleValue = 3.14159265
/
&CB
  Title = 'Hinge Offset'
  translationtype = 'timeindependent'
  translationvalue =0.0,.381,0.0
/
 &CB
  Title = 'Lead Lag Blade 3'
  iB = 2
  AngleType = 'nonperiodic'
  filename = '/OUTPUTS/Lagging_Angles_WOPWOP3.dat'
  Axistype = 'timeindependent'
  Axisvalue = 0.,0.,1.
/
 &CB
  Title = 'Flapping Blade 3'
  iB = 1
  Axistype = 'timeindependent'
  Axisvalue = 1.,0.,0.
  AngleType = 'nonperiodic'
  filename = '/OUTPUTS/Flapping_Angles_WOPWOP3.dat'

/
 &CB
  Title = 'Spar offset final'
  translationtype = 'timeindependent'
```

```
  translationvalue = 0.0,1.54091278,0.
/

&ContainerIn
  Title='Blade 4 Loading'
  patchGeometryFile='OUTPUTS/geometry_converter.dat'
  patchLoadingFile='OUTPUTS/forces_blade4.dat'
  nbBase=5
/
&CB
  Title='Offset for blade 4 (270 Degrees)'
  axisType='TimeIndependent'
  axisValue=0.0,0.0,1.0
  angleType='TimeIndependent'
  angleValue =4.71238898
/
&CB
  Title = 'Hinge Offset'
  translationtype = 'timeindependent'
  translationvalue =0.0,.381,0.0
/
 &CB
  Title = 'Lead Lag Blade 4'
  iB = 2
  AngleType = 'nonperiodic'
  filename = '/OUTPUTS/Lagging_Angles_WOPWOP4.dat'
  Axistype = 'timeindependent'
  Axisvalue = 0.,0.,1.
/
 &CB
  Title = 'Flapping Blade 4'
  iB = 1
  Axistype = 'timeindependent'
  Axisvalue = 1.,0.,0.
  AngleType = 'nonperiodic'
  filename = '/OUTPUTS/Flapping_Angles_WOPWOP4.dat'

/
 &CB
  Title = 'Spar offset final'
  translationtype = 'timeindependent'
  translationvalue = 0.0,1.54091278,0.

/
&ContainerIn
  Title = 'Auxillary Prop'
  !dTau = .0002084 !every  1 degree
  nbContainer = 2
  nbBase = 4
```

```
/
&CB
  Title ='To the back!'
  translationtype = 'timeindependent'
  translationValue = 11.07,0.0,-1.7 !m
/
&CB
  translationType='KnownFunction'
  VH = -102.889,0.0,0.0 !m/s

/
&CB
  Title="Rotate Aux Prop"
  axisType='TimeIndependent'
  axisValue=0.0,1.0,0.0
  angleType='TimeIndependent'
  angleValue =1.57079633
/

&CB
  Title="Angular Rotation"
  AngleType="KnownFunction"
  Omega=  200.99  !rad/s
  axisType='TimeIndependent'
  AxisValue=0.0,0.0,1.0
/

&Containerin
  Title = 'Thickness Prop Files'
  nbContainer = 7
/

&Containerin
  Title = 'Prop Blade 1'
  patchGeometryFile='OUTPUTS/ClarkYOut.wop'
  nbBase=1

/
 &CB
  Title='Prop Offset blade 1'
  axisType='TimeIndependent'
  axisValue=0.0,0.0,1.0
  angleType='TimeIndependent'
  angleValue =0.0
/
&Containerin
  Title = 'Prop Blade 2'
  patchGeometryFile='OUTPUTS/ClarkYOut.wop'
  nbBase=1
```

```
/
 &CB
   Title='Prop Offset blade 2'
   axisType='TimeIndependent'
   axisValue=0.0,0.0,1.0
   angleType='TimeIndependent'
   angleValue =.89759790
/
&Containerin
   Title = 'Prop Blade 3'
   patchGeometryFile='OUTPUTS/ClarkYOut.wop'
   nbBase=1

/
 &CB
   Title='Prop Offset blade 3'
   axisType='TimeIndependent'
   axisValue=0.0,0.0,1.0
   angleType='TimeIndependent'
   angleValue =1.79519580
/
&Containerin
   Title = 'Prop Blade 4'
   patchGeometryFile='OUTPUTS/ClarkYOut.wop'
   nbBase=1

/
 &CB
   Title='Prop Offset blade 4'
   axisType='TimeIndependent'
   axisValue=0.0,0.0,1.0
   angleType='TimeIndependent'
   angleValue =2.69279370
/
&Containerin
   Title = 'Prop Blade 5'
   patchGeometryFile='OUTPUTS/ClarkYOut.wop'
   nbBase=1

/
 &CB
   Title='Prop Offset blade 5'
   axisType='TimeIndependent'
   axisValue=0.0,0.0,1.0
   angleType='TimeIndependent'
   angleValue =3.59039160
/
&Containerin
```

```
  Title = 'Prop Blade 6'
  patchGeometryFile='OUTPUTS/ClarkYOut.wop'
  nbBase=1

/
 &CB
  Title='Prop Offset blade 6'
  axisType='TimeIndependent'
  axisValue=0.0,0.0,1.0
  angleType='TimeIndependent'
  angleValue =4.48798951
/
&Containerin
  Title = 'Prop Blade 7'
  patchGeometryFile='OUTPUTS/ClarkYOut.wop'
  nbBase=1

/
 &CB
  Title='Prop Offset blade 7'
  axisType='TimeIndependent'
  axisValue=0.0,0.0,1.0
  angleType='TimeIndependent'
  angleValue =5.38558741
  Title='Blade 1 Loading'
/
&Containerin
  Title = 'Loading Prop Files'
  nbContainer = 7
/
&Containerin
  Title = 'Prop Loading Blade 1'
  patchGeometryFile='OUTPUTS/PropGeometry.dat'
  patchLoadingFile='OUTPUTS/PropLoading.dat'
  nbBase=1
/
&CB
  Title='Offset for Prop blade 1 (0 Degrees)'
  axisType='TimeIndependent'
  axisValue=0.0,0.0,1.0
  angleType='TimeIndependent'
  angleValue =0
/
&Containerin
  Title = 'Prop Loading Blade 2'
  patchGeometryFile='OUTPUTS/PropGeometry.dat'
  patchLoadingFile='OUTPUTS/PropLoading.dat'
  nbBase=1
/
```

```
&CB
  Title='Offset for Prop blade 2 (0 Degrees)'
  axisType='TimeIndependent'
  axisValue=0.0,0.0,1.0
  angleType='TimeIndependent'
  angleValue =.89759790
/
&Containerin
  Title = 'Prop Loading Blade 3'
  patchGeometryFile='OUTPUTS/PropGeometry.dat'
  patchLoadingFile='OUTPUTS/PropLoading.dat'
  nbBase=1
/
&CB
  Title='Offset for Prop blade 3 (0 Degrees)'
  axisType='TimeIndependent'
  axisValue=0.0,0.0,1.0
  angleType='TimeIndependent'
  angleValue =1.7951958
/
&Containerin
  Title = 'Prop Loading Blade 4'
  patchGeometryFile='OUTPUTS/PropGeometry.dat'
  patchLoadingFile='OUTPUTS/PropLoading.dat'
  nbBase=1
/
&CB
  Title='Offset for Prop blade 4 (0 Degrees)'
  axisType='TimeIndependent'
  axisValue=0.0,0.0,1.0
  angleType='TimeIndependent'
  angleValue =2.69279370
/
&Containerin
  Title = 'Prop Loading Blade 5'
  patchGeometryFile='OUTPUTS/PropGeometry.dat'
  patchLoadingFile='OUTPUTS/PropLoading.dat'
  nbBase=1
/
&CB
  Title='Offset for Prop blade 5 (0 Degrees)'
  axisType='TimeIndependent'
  axisValue=0.0,0.0,1.0
  angleType='TimeIndependent'
  angleValue =3.59039160
/
&Containerin
  Title = 'Prop Loading Blade 6'
  patchGeometryFile='OUTPUTS/PropGeometry.dat'
```

```
  patchLoadingFile='OUTPUTS/PropLoading.dat'
  nbBase=1
/
&CB
  Title='Offset for Prop blade 6 (0 Degrees)'
  axisType='TimeIndependent'
  axisValue=0.0,0.0,1.0
  angleType='TimeIndependent'
  angleValue =4.48798951
/
&Containerin
  Title = 'Prop Loading Blade 7'
  patchGeometryFile='OUTPUTS/PropGeometry.dat'
  patchLoadingFile='OUTPUTS/PropLoading.dat'
  nbBase=1
/
&CB
  Title='Offset for Prop blade 7 (0 Degrees)'
  axisType='TimeIndependent'
  axisValue=0.0,0.0,1.0
  angleType='TimeIndependent'
  angleValue =5.38558741
/
```